

# Certifiable Black-Box Attacks with Randomized Adversarial Examples: Breaking Defenses with Provable Confidence

Hanbin Hong  
University of Connecticut  
Storrs, Connecticut, USA

Xinyu Zhang  
Zhejiang University  
Hangzhou, Zhejiang, China

Binghui Wang  
Illinois Institute of Technology  
Chicago, Illinois, USA

Zhongjie Ba  
Zhejiang University  
Hangzhou, Zhejiang, China

Yuan Hong  
University of Connecticut  
Storrs, Connecticut, USA

## ABSTRACT

Black-box adversarial attacks have shown strong potential to subvert machine learning models. Existing black-box attacks craft adversarial examples by iteratively querying the target model and/or leveraging the transferability of a local surrogate model. Recently, such attacks can be effectively mitigated by state-of-the-art (SOTA) defenses, e.g., detection via the pattern of sequential queries, or injecting noise into the model. To our best knowledge, we take the first step to study a new paradigm of black-box attacks with provable guarantees – certifiable black-box attacks that can guarantee the attack success probability (ASP) of adversarial examples before querying over the target model. This new black-box attack unveils significant vulnerabilities of machine learning models, compared to traditional empirical black-box attacks, e.g., breaking strong SOTA defenses with provable confidence, constructing a space of (infinite) adversarial examples with high ASP, and the ASP of the generated adversarial examples is theoretically guaranteed without verification/queries over the target model. Specifically, we establish a novel theoretical foundation for ensuring the ASP of the black-box attack with randomized adversarial examples (AEs). Then, we propose several novel techniques to craft the randomized AEs while reducing the perturbation size for better imperceptibility. Finally, we have comprehensively evaluated the certifiable black-box attacks on the CIFAR10/100, ImageNet, and LibriSpeech datasets, while benchmarking with 16 SOTA empirical black-box attacks, against various SOTA defenses in the domains of computer vision and speech recognition. Both theoretical and experimental results have validated the significance of the proposed attack.

## 1 INTRODUCTION

Machine learning (ML) models have achieved unprecedented success and have been widely integrated into many practical applications. However, it is well known that minor perturbations injected into the input data are sufficient to induce model misclassification [53]. Many state-of-the-art (SOTA) adversarial attacks [2, 7, 12, 14, 16, 39, 45, 53, 56, 83] have been proposed to explore the vulnerabilities of a variety of ML models. Wherein, the stringent *black-box* attack is believed to be closer to real-world security practice [14, 59]. In black-box attacks, the adversary only has access to the target ML model’s outputs (either prediction scores or hard labels). Through iteratively querying the target model, the adversary

progressively updates the perturbation until convergence. Existing black-box attack methods primarily utilize gradient estimation [5, 16, 19, 26, 39], surrogate models [25, 58, 59, 70], or heuristic algorithms [2, 7, 8, 31, 48] to generate adversarial perturbations.

Although these attack algorithms can empirically achieve relatively high attack success rates (e.g., on CIFAR-10 [44]), their query process is shown to be easy to detect or interrupt due to the minor perturbation changes and high reliance on the previous perturbation [13, 17, 47, 61]. For example, “Blacklight” [47] can achieve 100% detection rate on most of the existing black-box attacks by checking the similarity of queries; some “randomized defense” methods [13, 17, 34, 51, 61] inject random noise to the inputs, outputs, intermediate features or model parameters such that the performance of existing black-box attacks can be significantly degraded (since the query results are obfuscated to be unpredictable). To break such two types of SOTA defenses [17, 34, 47, 51, 61], it is challenging to design an effective attack equipped with both *high degree of randomness to bypass the strong detection* (e.g., Blacklight [47]) and *high robustness to resist randomized defense*. A feasible solution is to add random noise to the adversarial example by the adversary, but it will make the query intractable. Therefore, an innovative method is desirable to carefully craft the adversarial example based on feedback from queries using randomly generated inputs.

To this end, we propose a novel attack paradigm, termed *Certifiable Attack*, that ensures a provable attack success probability (ASP) on the randomized adversarial examples against the equipped defenses (or no defense). Specifically, our attack strategy integrates random noise into the queries while preserving the adversarial efficacy of these queries. In particular, we model the adversarial examples as a random variable in the input space following an underlying noise distribution  $\varphi$ , namely “*Adversarial Distribution*”. Then, we design a novel query strategy and establish the theoretical foundation to guarantee the ASP of the distribution throughout the crafting process. A novel framework is also developed to find the initial *Adversarial Distribution*, optimize it, and use it to sample the adversarial examples.

### 1.1 Certifiable Attacks vs. Empirical Attacks

Compared with existing empirical black-box attacks, the Certifiable Attack demonstrates multi-faceted advantages (also see Figure 1):

- (a) **Strong attack to break SOTA defenses.** The randomness in the certifiable attack allows it to effectively bypass detection methods that rely on the similarity between the attacker’s sequence of queries (e.g., Blacklight [47]), while traditional

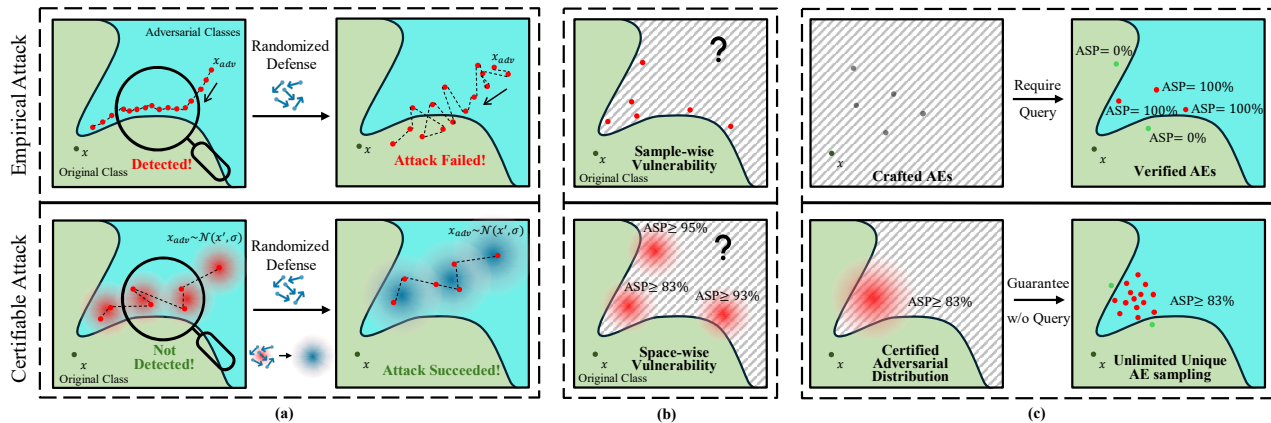


**Figure 1: Empirical attacks vs. Certifiable attacks. (a) Certifiable attack can break the SOTA AE detection and randomized defenses. (b) Certifiable attack uncovers space-wise vulnerability rather than sample-wise vulnerability. (c) Once certified, Certifiable Attack can generate unlimited unique AEs with a guaranteed minimum ASP without querying the model for verification, while the empirical attack requires verifying the attack result of crafted AE by query.**

empirical attacks often create a suspicious trajectory of highly similar perturbations. The certifiable attack also provides a provable guarantee of success for attacks using randomized inputs, by taking into account the equipped defense and target model, enhancing its resistance to randomized defense [13, 61].

- (b) **Adversarial space vs. Adversarial example (AE).** Distinct from traditional empirical adversarial attacks, which uncover model vulnerabilities with sample-wise inputs, the Certifiable Attack seeks to explore an adversarial input space constructed by an *Adversarial Distribution*. This continuous space facilitates the generation of numerous (potentially infinite) adversarial examples with a high ASP, thus revealing a more consistent and severe vulnerability of the target model.
- (c) **Adversarial Examples (AEs) sampled from the adversarial distribution are verification-free.** Empirical attacks search AEs by iteratively querying the target model and verifying the query outputs (*the final successful AE is also used to query over the target model; then it will be verified and recorded by the defender/target model*). Instead, the certifiable attack crafts the *adversarial distribution* with a guaranteed lower bound of the ASP. Due to the highly-dimensional and continuous input space, AEs sampled from the adversarial distribution can be considered as unique (with noise in all the dimensions) and have negligible probability of being recorded by the defender/target model after verification. The ASP of such AEs are theoretically guaranteed (verification-free), and they are new to the defender, posing more challenges for mitigation.

## 1.2 Randomization for Certifiable Attacks

To pursue certifiable attacks, we theoretically bound the ASP of *Adversarial Distribution* based on a novel way of utilizing randomized smoothing [22], a technique achieving great success in the certified defenses with probabilistic guarantees.

The design for the randomization-based certifiable attack follows an intuitive goal, i.e., *ensuring that the classification results are consistently wrong over the distribution*. However, many new significant challenges should be addressed. First, existing theories

(randomization for certified defenses, e.g., [22]) cannot be directly adapted to certifiable attacks since they have completely different goals and settings. Second, how to efficiently craft the *Adversarial Distribution* that can ensure the ASP is challenging since it requires maintaining the wrong prediction over a large number of randomized samples drawing from the distribution. Third, how to make the *Adversarial Distribution* as imperceptible as possible is also challenging due to their randomness. By addressing these new challenges, in this paper, we make the following significant contributions:

- 1) To our best knowledge, we introduce the first *certifiable attack theory* based on randomization for the black-box setting, which universally guarantees the attack success probability of AEs drawn from different noise distributions, e.g., Gaussian, Laplace, and Cauchy distributions, enabling a novel transition from deterministic to probabilistic adversarial attacks.
- 2) We propose a novel *certifiable attack framework* that can efficiently craft certifiable *Adversarial Distribution* with provable ASP and imperceptibility. Specifically, we design a novel *randomized parallel query method* to efficiently collect probabilistic query results from any target model, which supports the certifiable attack theory. We propose a novel *self-supervised localization* method as well as a binary-search localization method to efficiently generate certifiable *Adversarial Distribution*. We design a novel *geometric shifting* method to reduce the perturbation size for better imperceptibility while ensuring the ASP. Finally, we have validated that diffusion models [35] can be used to further denoise the randomized AEs with guaranteed ASP.
- 3) We comprehensively evaluate the performance of the certifiable attack with different settings on 4 datasets, while benchmarking with 16 SOTA empirical black-box attacks, against various defenses. Experimental results consistently demonstrate that our certifiable attack effectively breaks the SOTA defenses, including adversarial detection, randomized pre-processing and post-processing defenses, as well as adversarial training defenses

**Table 1: Comparison of state-of-the-art empirical black-box attacks with certifiable attack**

Black-box Attacks	Query Type	Perturbation Type	ASP Guarantee	vs. Detection on Attacker's Queries	vs. Randomized Pre-process. Defense	vs. Randomized Post-process. Defense
Bandit [40], NES [39], Parsimonious [55], Sign [1], Square [2], ZOSignSGD [50]	Score-based	$\ell_\infty$ -bounded	×	×	×	✓
GeoDA [62], HSJ [14], Opt [19], RayS [15], SignFlip [18], SignOPT [20]	Label-based	$\ell_\infty$ -bounded	×	×	×	×
Bandit [40], NES [39], Simple [31], Square [2], ZOSignSGD [50]	Score-based	$\ell_2$ -bounded	×	×	×	✓
Boundary [7], GeoDA [62], HSJ [14], Opt [19], SignOPT [20]	Label-based	$\ell_2$ -bounded	×	×	×	×
PointWise [68], SparseEvo [78]	Label-based	Optimized	×	×	×	×
Certifiable Attack (ours)	Label-based	Optimized	✓	✓	✓	✓

(Also, Table 1 shows a summary of the certifiable attack vs. SOTA black-box attacks).

## 2 PROBLEM DEFINITION

**Threat Model:** We consider designing a certifiable attack where the target model may or may not be protected by a defense mechanism.

- **Adversary:** We focus on the hard-label black-box attack, where the adversary only knows the predicted label by querying the target ML model. The adversary's objective is to craft adversarial examples to fool the model based on the query results.
- **Model Owner:** The model owner pursues the model utility. We consider three different levels of the model owner's knowledge and capability: 1) The model owner has no awareness of the adversarial attacks and is not equipped with any defense; 2) The model owner is aware of the adversarial attack but has no knowledge of the attack method. The model owner can deploy general defense methods such as adversarial training [53]; 3) The model owner is aware of the adversarial attack and has knowledge about the attack method. The model owner can deploy adaptive defenses that are specifically designed for the attack.

**Problem Formulation:** We first briefly review adversarial examples, and then formally define our problem. Given an ML classifier  $f$  and a testing data  $x \in \mathbb{R}^d$  with label  $y$  from a label set  $\mathcal{Y} = [1, \dots, C]$  (where  $C$  is the number of classes). An adversary carefully crafts a perturbation on the data  $x$  such that the classifier  $f$  misclassifies the perturbed data  $x_{adv}$ , i.e.,  $f(x_{adv}) \neq y$  under  $x_{adv} \in [\Pi_a, \Pi_b]^d$ , where  $[\Pi_a, \Pi_b]^d$  is the valid input space. The perturbed data  $x_{adv}$  is called *adversarial example*. Imperceptibility is usually achieved by restricting the  $\ell_2$  or  $\ell_\infty$  norm of the perturbation  $x_{adv} - x$ , or by minimizing the magnitude of this perturbation.

In the black-box setting, an adversary can use *empirical* black-box attack techniques (details in Section 6) to iteratively query the classifier  $f$  and progressively update the perturbation until finding a successful adversarial example for a testing example. However, such attack strategies have key limitations: 1) query inefficient, usually  $> 100$  queries per adversarial example; 2) easy to be detected by observing the query trajectory [13, 17, 47, 61]; and 3) lack of guaranteed attack performance, i.e., cannot provably guarantee a (un)successful adversarial example under a given budget.

We aim to address all these limitations and design an efficient and effective certifiable black-box attack in the paper. Particularly, instead of inefficiently searching adversarial *examples* one-by-one, we want to certifiably find the underlying adversarial *distribution* that the adversarial examples lie on.

**Definition 2.1 (Certifiable black-box attack).** Given a classifier  $f: \mathbb{R}^d \rightarrow \mathcal{Y}$ , a clean input  $x \in \mathbb{R}^d$  with label  $y \in \mathcal{Y}$ , and an Attack

Success Probability Threshold  $p$ , the certifiable attack is to find an *Adversarial Distribution*  $\varphi(x', \kappa)$  with mean  $x'$  and parameters  $\kappa^1$ , such that data sampled from  $\varphi$  have at least  $p$  probability of being misclassified (i.e., adversarial examples). That is,

$$\mathbb{P}_{x_{adv} \sim \varphi(x', \kappa)} [f(x_{adv}) \neq y] \geq p \quad (1)$$

$$\text{s.t. } x_{adv} \in [\Pi_a, \Pi_b]^d. \quad (2)$$

**Design Goals:** We expect our attack to achieve the below goals.

- 1) **Certifiable:** It can provide provable guarantees on the minimum attack success probability of the crafted adversarial examples.
- 2) **Verification free:** It can not only verify examples to be adversarial *after* querying the model, but also verify examples *before* the query by giving its ASP. This significantly boosts the effectiveness of adversarial examples generation.
- 3) **Query efficient:** It needs as few number of queries as possible. Fewer queries can definitely save the adversary's cost.
- 4) **Bypass defenses:** It can generate imperceptible adversarial perturbations that can bypass the existing detection and pre/post-processing based defenses [13, 17, 47, 61].

## 3 ATTACK OVERVIEW

At a high level, our certifiable black-box attack can be divided into three phases. The overview of our attack is depicted in Figure 2.

**Phase I: Adversarial Distribution Localization.** This phase initially locates a feasible *Adversarial Distribution*  $\varphi$  with guarantees on the lower bound of attack success probabilities (i.e., satisfying Eq. (1)). There are a few challenges. First, computing the exact probability  $\mathbb{P}[f(x_{adv}) \neq y]$  is intractable due to the high-dimensional continuous input space. Second, due to the black-box nature, there exists no gradient information that can be used. To address the first challenge and ensure query efficiency, we propose a Randomized Parallel Query (RPQ) strategy that can approximate the probability and ensure multiple queries be implemented in parallel. To address the second challenge, we design two localization strategies to enable learning a feasible adversarial distribution. The first strategy adapts the existing self-supervised perturbation (SSP) technique [58], which facilitates designing a classifier-unknown loss on a pretrained feature extractor such that the adversarial examples/perturbations can be optimized. The second one is based on binary search. It first randomly initializes a qualified *Adversarial Distribution*, and then reduces the perturbation size using the binary search algorithm. See Section 4.1 for more details.

<sup>1</sup>If  $\varphi$  is a Gaussian distribution,  $\kappa$  is the standard deviation of  $\varphi$ . If  $\varphi$  is a Generalized normal distribution,  $\kappa = (a, b)$ , with  $a$  and  $b$  the scale and shape parameters of  $\varphi$ , respectively. Notice that, the distribution will be applied to all the dimensions in the input, and *Adversarial Distribution* is a noise distribution over the input space.

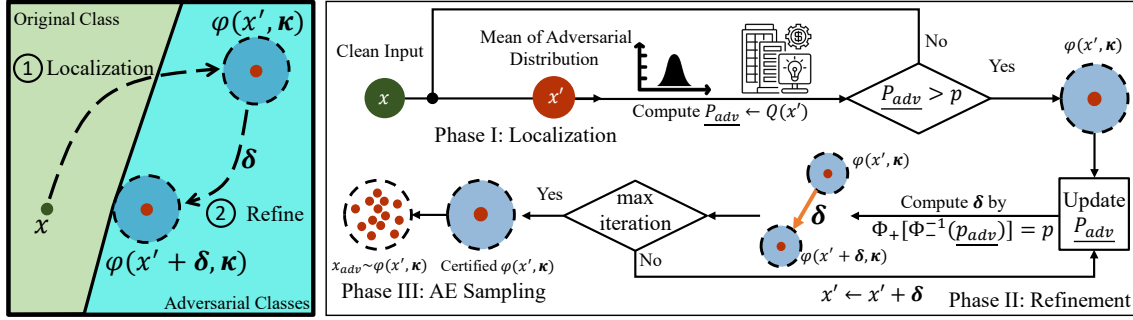


Figure 2: Overview of our certifiable black-box attack to generate certified *Adversarial Distribution*.

**Phase II: Adversarial Distribution Refinement.** While successfully generating the adversarial distribution, the adversarial examples from it often induce relatively large perturbation sizes. This phrase further refines the adversarial distribution by reducing the perturbation size, and maintains the guarantee of attack success probability as well. Particularly, we propose to shift the adversarial distribution close to the decision boundary of the classifier. This problem can be solved by two steps: *the first step finds the shifting direction, and the second step derives the shifting distance and maintains the guarantee.* We design a novel shifting method to find the local-optimal *Adversarial Distribution* by considering the geometric relationship between the decision boundary and *Adversarial Distribution*. Deciding the shifting distance can then be converted to an optimization problem. We then propose a binary search algorithm to achieve the goal. See Section 4.2 for more details.

**Phase III: Adversarial Example Sampling.** Phases I and II craft an *Adversarial Distribution* with guaranteed attack success probability, called “certifiable attack”. To transform the *Adversarial Distribution* into concrete AEs, we need to sample the AE from the *Adversarial Distribution*. The sampled AEs naturally maintain the certified ASP without the need for additional model queries. Optionally, the adversary can verify the success of these sampled AEs to ensure a successful attack, turning the certifiable attack into an empirical attack. Specifically, the adversary can sequentially sample the adversarial examples from *Adversarial Distribution* and query the target model until finding the successful adversarial example(s).

## 4 CERTIFIABLE BLACK-BOX ATTACK

In this section, we present our certifiable black-box attack in detail. We first introduce the Randomized Parallel Query strategy that estimates the lower bound probability of being the adversarial example (Section 4.1.1). We then develop two algorithms to locate the feasible *Adversarial Distribution* (Section 4.1.2). Next, we propose our refinement method to reduce the perturbation size, while maintaining the guarantees of attack success probability (Section 4.2). We also provide the theoretical analysis of the convergence and confidence bound of the Shifting method.

### 4.1 Adversarial Distribution Localization

**4.1.1 Randomized Parallel Query.** As stated, computing the exact probability  $\mathbb{P}[f(x_{adv}) \neq y]$  with  $x_{adv} \sim \varphi(x', \kappa)$  is intractable. Here, we propose to estimate its low bound probability by the Monte Carlo method. This requires the adversary to query the classifier

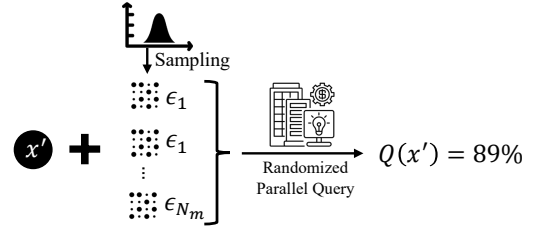


Figure 3: Illustration of Randomized Parallel Query—It returns the probability  $Q(x')$  that  $x' + \epsilon$  is an adversarial example.

#### Algorithm 1 Lower Bound of Attack Success Probability

**Input:** Mean  $x'$  of the *Adversarial Distribution*  $\varphi$ , classifier  $f$ , confidence level  $\alpha$ , Monte Carlo samples  $N_m$ , ground truth label  $y$ .  
**Output:** The lower bound of attack success probability  $\underline{p}_{adv}$   
1:  $\epsilon_1, \epsilon_2, \dots, \epsilon_{N_m} \sim \varphi(0, \kappa)$   
2: Incorrect prediction count  $k \leftarrow \sum_{i=1}^{N_m} \mathbb{1}[f(x' + \epsilon_i) \neq y]$   
3: **return**  $\underline{p}_{adv} \leftarrow \text{LOWERCONFBOUND}(k, N_m, 1 - \alpha)$

with random instances sampled from an *Adversarial Distribution*. By noting that random instances can be queried efficiently in parallel, we propose the Randomized Parallel Query (RPQ) to compute the lower bound of the attack success probability as below:

$$\begin{aligned} Q(x') &= \underline{p}_{adv} \leq \mathbb{P}_{x_{adv} \sim \varphi(x', \kappa)} [f(x_{adv}) \neq y] \\ &= \mathbb{P}_{\epsilon \sim \varphi(0, \kappa)} [f(x' + \epsilon) \neq y]. \end{aligned} \quad (3)$$

With a given  $x'$ , the lower bound probability  $\underline{p}_{adv}$  can be estimated via the Binomial testing on a zero-mean distribution  $\varphi(0, \kappa)$  using Clopper-Pearson confidence interval [46] following the Algorithm 1, where the  $\text{LOWERCONFBOUND}(k, N_m, 1 - \alpha)$  returns the one-sided  $(1 - \alpha)$  lower confidence interval.

Now we can estimate  $\underline{p}_{adv}$  given an *Adversarial Distribution* with known mean/location  $x'$ . The next question is how to decide  $x'$  to satisfy Eq. (1), i.e., locating the adversarial distribution that includes certifiable adversarial examples (with probability at least  $p$ ).

The simplest way is random localization, where the input  $x$  is uniformly sampled from the input space  $[\Pi_a, \Pi_b]^d$ , e.g.,  $[0, 1]^d$ , followed by the RPQ to check if  $\underline{p}_{adv}$  is larger than  $p$ . However, random localization could not generate a good initial adversarial distribution due to the high-dimensional input space. Below we propose two practical localization methods to mitigate the issue.

---

**Algorithm 2** Smoothed Self-Supervised Perturbation (SSSP)
 

---

**Input:** Clean input  $x$ , feature extractor  $\mathcal{F}$ , noise distribution  $\varphi(0, \kappa)$ , maximum iterations  $n_{max}$ , perturbation budget  $\pi$ , step size  $\eta$ , and noise sampling number  $N_s$ .

**Output:** Updated mean  $x'$  of *Adversarial Distribution*

```

1:  $x' = x$ 
2: for  $n = 1$  to  $n_{max}$  do
3:    $\mathcal{L}(x') \leftarrow \frac{1}{N_s} \sum_i^{N_s} [\|\mathcal{F}(x' + \epsilon_i) - \mathcal{F}(x + \epsilon_i)\|_2]$ ,  $\epsilon_i \sim \varphi$ 
4:    $x' \leftarrow x' + \eta \operatorname{sgn}(\nabla_{x'} \mathcal{L})$ 
5:    $x' \leftarrow \operatorname{Clip}(x', x - \pi, x + \pi)$ 
6:    $x' \leftarrow \operatorname{Clip}(x', 0.0, 1.0)$  (if  $x$  is an image)
7: return  $x'$ 
    
```

---



---

**Algorithm 3** Smoothed SSP for Certifiable Attack Localization
 

---

**Input:** Clean input  $x$ , feature extractor  $\mathcal{F}(\cdot)$ , RPQ function  $Q(\cdot)$ , smoothed SSP algorithm  $\text{SSSP}(\cdot)$  (Algorithm 2), initial perturbation budget  $\pi_{init}$ , step size  $\gamma$ , ASP Threshold  $p$ , maximum iterations  $N_{max}$ .

**Output:** Mean  $x'$  of *Adversarial Distribution*  $\varphi$ , number of RPQs  $q$ .

```

1:  $x' = x$ ,  $\pi = \pi_{init}$ ,  $N = 0$ ,  $q = 0$ 
2: while  $Q(x') < p$  and  $N < N_{max}$  do
3:    $N \leftarrow N + 1$ ,  $q \leftarrow q + 1$ ,  $\pi \leftarrow \pi + \gamma$ 
4:    $x' \leftarrow \text{SSSP}(x', \mathcal{F}, \pi)$ 
5: if  $Q(x') < p$  then
6:   return Abstain
7: else
8:   return  $x'$  and  $q$ 
    
```

---

**4.1.2 Proposed Localization Algorithms.** We notice the adversarial distribution localization is similar to empirical black-box attacks on generating adversarial examples. Here, we propose to adapt these empirical attack algorithms and design two localization algorithms.

**Smoothed Self-Supervised Localization:** To better locate the *Adversarial Distribution*, we propose to adapt the self-supervised perturbation (SSP) technique [58]. Specifically, SSP generates generic adversarial examples by distorting the features extracted by a pre-trained feature extractor on a large-scale dataset in a self-supervised manner. The rationale is that the extracted (adversarial) features can be transferred to other classifiers as well.

As our attack uses RPQ, we compute the feature distortion over a set of random samples from the *Adversarial Distribution*. Formally,

$$\begin{aligned}
 x' &= \arg \max_{x'} \mathbb{E}_{\epsilon \sim \varphi(0, \kappa)} [\|\mathcal{F}(x' + \epsilon) - \mathcal{F}(x + \epsilon)\|_2] \\
 \text{s.t. } &\|x' - x\|_\infty \leq \pi
 \end{aligned} \tag{4}$$

where  $\mathcal{F}$  is a pre-trained feature extractor. The perturbation budget  $\pi$  is initially set to a small value and later increased in multiple attempts of localization, ensuring that smaller perturbations are identified first. This optimization problem can be solved via the Projected Gradient Ascent method [53]. Let the adversarial loss be  $\mathcal{L}(x') \equiv \mathbb{E}_{\epsilon \sim \varphi} [\|\mathcal{F}(x' + \epsilon) - \mathcal{F}(x + \epsilon)\|_2]$ . Then we can locate the *Adversarial Distribution* via iteratively update  $x'$  with  $x' = x' + \eta \operatorname{sgn}(\nabla_{x'} \mathcal{L})$ , where  $\operatorname{sgn}(\cdot)$  is the sign function, and  $\eta$  denotes the step size. The details for localizing the *Adversarial Distribution* are summarized in Algorithms 2 and 3.

**Binary Search Localization:** Another method is to randomly initialize the location of *Adversarial Distribution* such that  $\underline{p}_{adv} \geq p$ ,

---

**Algorithm 4** Binary Search for Certifiable Attack Localization
 

---

**Input:** Clean input  $x$ , RPQ function  $Q(\cdot)$ , ASP Threshold  $p$ , random search iterations  $N_r$ , and binary search iteration  $N_b$ , error tolerance  $\Omega$ .

**Output:** Mean of initial *Adversarial Distribution*  $x'$ , number of RPQs  $q$ .

```

1:  $n = 0$ ,  $m = 0$ ,  $q = 0$ ,  $x^* = x$ 
2: while  $Q(x') < p$  and  $n \leq N_r$  do
3:    $x' \sim \text{Uniform}([0, 1]^d)$ 
4:    $q \leftarrow q + 1$ ,
5: if  $n > N_r$  then return Abstain
6: while  $m < N_b$  and  $\|x' - x^*\|_2 \leq \Omega$  do
7:   if  $Q(\frac{x^* + x'}{2}) \geq p$  then
8:      $x' = \frac{x^* + x'}{2}$ 
9:   else
10:     $x^* = \frac{x^* + x'}{2}$ 
11: return  $x'$ 
    
```

---

and then reduce the gap between  $\underline{p}_{adv}$  and  $p$ , as well as the perturbation via binary search. The algorithm is presented in Algorithm 4. This method is efficient in reducing the perturbation size once the feasible *Adversarial Distribution* is found by random search. Appendix C visualizes some  $x_{adv}$  during the crafting process for both Binary Search Localization and SSSP Localization.

## 4.2 Adversarial Distribution Refinement

Though our localization algorithms can find an effective *Adversarial Distribution*, our empirical results found the perturbation size can be large (See Table 5.4.3). This occurs possibly because the pretrained feature extractor is too generic and the generated adversarial perturbation is suboptimal for our target classifier. To mitigate the issue, we propose to reduce the perturbation by refining the *Adversarial Distribution* while still maintaining the condition Eq. (1).

Our key observation is that the optimal perturbation is achieved when the adversarial example is close to the decision boundary of the target classifier. Hence, we propose to shift the *Adversarial Distribution* until intersecting the decision boundary, thereby locating the locally optimal point on that boundary.

**4.2.1 Certification for Adversarial Distribution Shifting.** We propose a theory on shifting the *Adversarial Distribution* while maintaining the attack success probability. We denote  $\varphi(x' + \delta, \kappa)$  as a shifted distribution for the *Adversarial Distribution*  $\varphi(x', \kappa)$  by a shifting vector  $\delta$ . Then, the shifted *Adversarial Distribution* ensures the ASP if  $\delta$  satisfies the condition presented in Theorem 1.

**THEOREM 1. (Certifiable Adversarial Distribution Shifting)** Let  $f$  be a classifier,  $\epsilon$  be the noise drawn from any continuous probability density function  $\varphi(0, \kappa)$ . Let  $p$  be the predefined attack success possibility threshold. Denote  $\underline{p}_{adv}$  as the lower bound of the attack success probability. For any  $x'$  satisfies

$$\mathbb{P}[f(x' + \epsilon) \neq y] \geq \underline{p}_{adv} = Q(x') \geq p, \tag{5}$$

$\mathbb{P}[f(x' + \delta + \epsilon) \neq y] \geq p$  is guaranteed for any shifting vector  $\delta$  when

$$\Phi_+[\Phi_-^{-1}(\underline{p}_{adv})] \geq p \tag{6}$$

where  $\Phi_-^{-1}$  is the inverse cumulative density function (CDF) of the random variable  $\frac{\varphi(\epsilon - \delta, \kappa)}{\varphi(\epsilon, \kappa)}$ , and  $\Phi_+$  the CDF of random variable  $\frac{\varphi(\epsilon, \kappa)}{\varphi(\epsilon + \delta, \kappa)}$ .

**PROOF.** See detailed proof in Appendix A.1.  $\square$

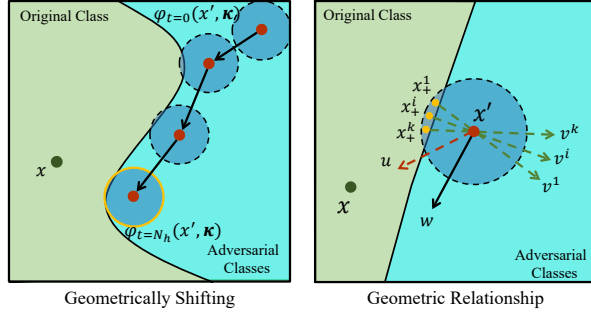


**Figure 4: Illustration of geometrically shifting.**

Theorem 1 ensures the minimum attack success probability if Eq. (5) and Eq. (6) hold while without querying  $\varphi(x' + \delta, \kappa)$ . Eq. (5) requires finding a  $x'$  such that the RPQ on samples of  $\varphi(x', \kappa)$  returns a  $p_{adv} \geq p$ , and Eq. (6) ensures any  $\delta$  meeting this condition will not reduce the attack success probability of the shifted *Adversarial Distribution* below  $p$ . Further, Theorem 1 works for any continuous noise distributions, e.g., Gaussian, Laplace, Exponential, and mixture PDFs. We also present the case when the noise is Gaussian in Corollary 2.1 in Appendix A.2. It shows the shifting perturbation  $\delta$  should satisfy  $\|\delta\|_2 \leq \sigma[\Phi^{-1}(p_{adv}) - \Phi^{-1}(p)]$ , where  $\Phi^{-1}$  is the inverse of Gaussian CDF.

**4.2.2 Obtaining Refined Adversarial Distribution.** Since the *Adversarial Distribution* can be shifted by any  $\delta$  satisfying Eq. (6), we propose to shift it toward the clean input with the maximum  $\delta$  that does not break the guarantee. By iteratively executing the RPQ and applying the Theorem 1, the *Adversarial Distribution* can be repeatedly shifted with a guarantee until approaching the decision boundary (where  $p_{adv} = p$ ).

The problem of shifting the *Adversarial Distribution* to reduce the perturbation can be solved by two steps: *first finding the shifting direction, and then deriving the shifting distance while maintaining the guarantee*. Here, we design a novel shifting method to find the locally optimal *Adversarial Distribution* by considering the geometric relationship between the decision boundary and the *Adversarial Distribution*, which is called “Geometrical Shifting”. Specifically, through using the noisy samples of *Adversarial Distribution* to “probe” the decision boundary, we shift the RandAE along the decision boundary and towards the clean input until finding the local optimal point on the decision boundary (see Figure 4 for the illustration). If none of the noisy samples can approach the decision boundary, we simply shift the *Adversarial Distribution* directly toward the clean input without considering the decision boundary.

**Finding the Shifting Direction:** The geometrical relationship is presented on the right-hand side of Figure 4. Denote  $x'$  as the mean of the current *Adversarial Distribution. When sampling the adversarial examples from the *Adversarial Distribution*, we mark the failed adversarial examples as  $x_+^1, x_+^2, \dots, x_+^i, \dots, x_+^k$ , aka., “samples fell into the original class”. The normalized vector from  $x_+^i$  to  $x'$  is denoted as  $v^i$ . The normalized vector from  $x'$  to  $x$  is denoted as  $u$ . If the *Adversarial Distribution* has no samples crossing the decision boundary, then we can shift the *Adversarial Distribution* straight toward the clean input (along the direction of  $u$ ) until it intersects the decision boundary, otherwise, the shifting should be along the*

---

### Algorithm 5 Shifting Direction

---

**Input:** Mean of the *Adversarial Distribution*  $x'$ , clean input  $x$ , vectors  $\{v^i\}$ , a vector  $u$ , maximum iteration  $M$ , updating step size  $\eta'$ .

**Output:** The shifting direction  $w$

```

1: Initialize  $w$  with random noise
2: if  $\{v^i\}$  is empty then
3:    $w = x - x'$ 
4: else
5:   for  $j = 1$  to  $M$  do
6:      $w \leftarrow w + \eta' \operatorname{sgn}[\nabla_w(\sum_{i=1}^k \sin(v^i, w) + \cos(u, w))]$ 
7:      $w \leftarrow \frac{w}{\|w\|_2}$ 
8:   return  $w$ 

```

---



---

### Algorithm 6 Shifting Distance

---

**Input:** Mean of *Adversarial Distribution*  $x'$ , noise distribution  $\varphi$ , randomized query function  $Q(\cdot)$ , the shifting direction algorithm  $SD(\cdot)$  (Algorithm 5), error threshold  $\epsilon$ , ASP Threshold  $p$ .

**Output:** The shifting perturbation  $\delta$

```

1:  $w \leftarrow SD(x'), p_{adv} \leftarrow Q(x')$ 
2: find a scalar  $a$  such that  $\delta = aw$  and  $\Phi_+[\Phi^{-1}(p_{adv})] > p$ 
3: find a scalar  $b$  such that  $\delta = bw$  and  $\Phi_+[\Phi^{-1}(p_{adv})] < p$ 
4: while  $\Phi_+[\Phi^{-1}(p_{adv})] < p$  or  $> p + \epsilon$  and  $n \leq N_k$  do
5:   if  $\Phi_+[\Phi^{-1}(p_{adv})] > p$  then
6:      $a \leftarrow \frac{(a+b)}{2}$ 
7:   else
8:      $b \leftarrow \frac{(a+b)}{2}$ 
9:    $\delta \leftarrow \frac{(a+b)}{2} w, n \leftarrow n + 1$ 
10: return  $\delta$ 

```

---



---

### Algorithm 7 Certifiable Attack Shifting

---

**Input:** Mean of *Adversarial Distribution*  $x'$ , noise distribution  $\varphi$ , randomized query function  $Q(\cdot)$ , shifting distance algorithm  $\text{SHIFT}(\cdot)$  (Algorithm 6), distance threshold  $\epsilon_s$ , ASP Threshold  $p$ , max iteration  $N_h$ .

**Output:** The shifted mean  $x'$

```

1:  $p_{adv} \leftarrow Q(x'), \delta \leftarrow \text{SHIFT}(x'), n = 0$ 
2: while  $p_{adv} > p$  and  $\|\delta\|_2 \geq \epsilon_s$  and  $n \leq N_h$  do
3:    $x' \leftarrow x' + \delta, p_{adv} \leftarrow Q(x'), \delta \leftarrow \text{SHIFT}(x'), n \leftarrow n + 1$ 
4:   if  $\|x' - x\|_2 \leq \|\delta\|_2$  then return  $x'$ 
5: return  $x'$ 

```

---

decision boundary but not cross it (without changing the certifiable attack guarantee). Note that the input space is high-dimensional, thus there could be many directions along the decision boundary. To reduce the perturbation, the direction should be similar to the vector  $u$  as much as possible. Based on these geometric analyses, the goals of the geometrical shifting can be summarized as: *The shifting direction should lie relatively parallel to the direction of  $u$ ; and be relatively vertical to the vectors  $v^i$ .*

Formally, denoting the shifting direction as  $w$ , then the goal of finding the shifting direction can be formulated as:

$$w = \arg \max \sum_{i=1}^k \sin(v^i, w) + \cos(u, w) \quad (7)$$

where  $\sin(\cdot)$  and  $\cos(\cdot)$  denote the sine and cosine function, and Eq. (7) can be solved via the gradient ascent algorithm.

**Calculating the Shifting Distance:** The shifting distance can be determined by maximizing  $\|\delta\|_2$  that satisfies the constraint of Eq. (6), i.e., when the equality holds. We use binary search to approach the equality and the Monte Carlo method to estimate the CDF of random variable  $\frac{\varphi(\epsilon-\delta, \kappa)}{\varphi(\epsilon, \kappa)}$  and  $\frac{\varphi(\epsilon, \kappa)}{\varphi(\epsilon+\delta, \kappa)}$ , similar to [37]. Algorithm 5, 6, and 7 show the details of finding the shifting direction, shifting distance, and the shifting process, respectively.

**Convergence Guarantee and Confidence Bound:** Any  $\delta$  computed by Algorithm 6 will satisfy the certifiable attack guarantee since it strictly ensures  $\Phi_+[\Phi_-^{-1}(p_{adv})] \geq p$ . Further, with a centralized noise distribution, the shifting algorithm is guaranteed to converge once the located *Adversarial Distribution* is feasible.

**THEOREM 2.** *If the PDF of noise distribution  $\varphi(x)$  decreases as the  $|x|$  increases, with the satisfaction of Eq. (5), given any direction vector  $w$ , the Shifting Distance algorithm guarantees to find  $\delta$  such that  $\Phi_+[\Phi_-^{-1}(p_{adv})] = p$  with confidence  $(1 - \alpha)(1 - 2e^{-2N_m\Delta^2})^2$ , where  $(1 - \alpha)$  is the confidence for of estimating  $p_{adv}$ ,  $N_m$  is the Monte Carlo samples, and  $\Delta$  is the error bound for the CDF estimation.*

PROOF. See detailed proof in Appendix A.3.  $\square$

### 4.3 Discussions on Our Attack

**Realizing Our Certifiable Attack:** Our certifiable attack does not have extra requirements on realization compared to empirical black-box attacks. To implement our attack, we only need to predefine a continuous noise distribution and a threshold of certified attack success probability. The adversary then adds the noise sampled from the distribution to the inputs and query the target model. Then, *Adversarial Distribution* can be crafted by RPQ and our theory.

**Randomized Query vs. Deterministic Query:** The proposed randomized query returns a *probability* over a batch of inputs with injected random noises, while the traditional query returns a *deterministic* output (score or hard label) from the target model. This probability return can provide more information that better guides the attack. In addition, the randomized queries can be executed in parallel for query acceleration. See results in Section 5.3.

**Imperceptibility with Diffusion Denoiser:** The certifiable adversarial examples sampled from *Adversarial Distribution* are noise-injected inputs that still might be perceptible when the noise is large. We can further leverage the recent innovation for image synthesis, i.e., diffusion model [35], to denoise the adversarial examples for better imperceptibility. The key idea is to consider the noise-perturbed adversarial examples as the middle sample in the forward process of the diffusion model [11, 88]. This is shown to improve the imperceptibility and the diversity of the adversarial examples. More technical details are shown in Appendix B and results in Table 38 in Appendix D.4.

**Extension to Certifiable White-Box Attacks:** Our certifiable attack can be easily extended to the white-box setting by adapting/designing a white-box localization method. Specifically, the Smoothed SSP localization method can directly compute the gradients of the noise-perturbed examples rather than leveraging the feature extractor, which may significantly improve the certified accuracy of the certifiable attack.

**Table 2: Summary of Experiments**

Experiments	Dataset	Model	Reference
Comparison with empirical attacks against Blacklight detection	CIFAR10	VGG16	Table 13
	CIFAR10	ResNet110	Table 14
	CIFAR10	ResNext29	Table 15
	CIFAR10	WRN28	Table 16
	CIFAR100	VGG16	Table 17
	CIFAR100	ResNet110	Table 18
	CIFAR100	ResNext29	Table 19
	CIFAR100	WRN28	Table 20
	ImageNet	ResNet18	Table 3
	Comparison with empirical attacks against RAND pre-processing defense	CIFAR10	VGG16
CIFAR10		ResNet110	Table 22
CIFAR10		ResNext29	Table 23
CIFAR10		WRN28	Table 24
CIFAR100		VGG16	Table 25
CIFAR100		ResNet110	Table 26
CIFAR100		ResNext29	Table 27
CIFAR100		WRN28	Table 28
ImageNet		ResNet18	Table 4
Comparison with empirical attacks against RAND post-processing defense		CIFAR10	VGG16
	CIFAR10	ResNet110	Table 30
	CIFAR10	ResNext29	Table 31
	CIFAR10	WRN28	Table 32
	CIFAR100	VGG16	Table 33
	CIFAR100	ResNet110	Table 34
	CIFAR100	ResNext29	Table 35
	CIFAR100	WRN28	Table 36
	ImageNet	ResNet18	Table 5
	Comparison with empirical attack against adversarial training	CIFAR10	ResNet110 ( $\ell_2$ )
CIFAR10		ResNet110 ( $\ell_\infty$ )	
Ablation: CA vs. different noise variance	CIFAR10	ResNet110	Table 7
	ImageNet	ResNet50	
Ablation: CA vs. different p	CIFAR10	ResNet110	Table 8
	ImageNet	ResNet50	
Ablation: CA vs. different Localization/Shifting	CIFAR10	ResNet110	Table 9
	ImageNet	ResNet50	
	LibriSpeech	ECAPA-TDNN	
Ablation: CA vs. different noise PDF	CIFAR10	ResNet110	Table 10
	ImageNet	ResNet50	
Ablation: CA w/ and w/o Diffusion Denoise	CIFAR10	ResNet110	Table 38
	ImageNet	ResNet50	
CA vs. Feature Squeezing	CIFAR10	ResNet110	Figure 8
CA vs. Adaptive Denoiser	CIFAR10	ResNet110	Table 11
CA vs. Rand. Smoothing	CIFAR10	ResNet110	Table 37

**Extension to Targeted Certifiable Attack:** Our attack design focuses on the untargeted certifiable attack. It can also be generalized to the targeted attack setting, where we require the majority of the noise-perturbed inputs be *certifiably* misclassified to a specific *target* label. However, we admit it would be more challenging to find a successful *Adversarial Distribution* in this scenario.

## 5 EVALUATIONS

We comprehensively evaluate our certifiable black-box attack in various experimental settings. Particularly, we would like to study the following research questions:

- **RQ1:** How effective is the learnt *Adversarial Distribution*? Particularly, how large is the probability of samples from it being successful adversarial examples?
- **RQ2:** Can our certifiable attack outperform empirical attacks in terms of attack effectiveness and query efficiency?
- **RQ3:** How effective is our attack to break SOTA defenses?
- **RQ4:** What is the impact of the design components and their hyperparameters on our attack?

Accordingly, we first assess the empirical attack success possibility of the *Adversarial Distribution* in Section 5.2. Then, we evaluate our certifiable attack on various models with defenses while benchmarking with empirical black-box attacks in Section 5.3. In Section 5.4, we conduct ablation studies to explore in-depth our certifiable attack. *All experiments are summarized in Table 2 for reference.*

## 5.1 Experimental Setup

**Datasets and Models.** We use three benchmark datasets for image classification: CIFAR10/CIFAR100 [44] and ImageNet [66]. CIFAR10 and CIFAR100, both consisting of 60,000 32x32 color images split into 10 and 100 classes, respectively. ImageNet is a large-scale dataset with 1,000 classes. The training set contains 1,281,167 images and the validation set contains 50,000 images (resized to  $3 \times 224 \times 224$ ). we use VGG [71], ResNet [33], ResNext [82], and WRN [86] as the target model. We use a pre-trained ResNet34 on ImageNet as the feature extractor (in the Smoothed SSP localization). We also test our attacks on the audio dataset LibriSpeech [43] for the speaker verification task, and results are shown in Appendix D.5.

**Baseline Attacks.** We compare our certifiable (hard label-based) black-box attack with SOTA black-box attacks including 7 *hard label-based* black-box attacks: GeoDA [62], HSJ [14], Opt [19], RayS [15], SignFlip [18], SignOPT [20], and Boundary [7]; and 7 *score-based* black-box attacks: Bandit [40], NES [39], Parsimonious [55], Sign [1], Square [2], ZOSignSGD [50], Simple attack [31]. As our method does not constrain the perturbation budget but minimizing the perturbation, we also compare with two similar attacks: SparseEvo [78] and PointWise [68]. We evaluate our attack with both SSSP localization and binary-search localization. For optimization-based attacks, we limit the AEs in the valid image space. For a fair comparison with optimization-based attacks, the perturbation budget for  $\ell_p$ -bounded attacks are set to 0.1 for  $\ell_\infty$  and 5 for  $\ell_2$  on CIFAR10 and CIFAR100, while on ImageNet, they are  $\ell_\infty = 0.1$  and  $\ell_2 = 40$ . The maximum query limits are 10,000 for CIFAR10 and CIFAR100 and 1,000 for ImageNet. We evaluate 1,000 randomly selected images for each dataset.

**Defenses.** We select 4 SOTA defenses against black-box attacks for evaluation: Blacklight detection [47], Randomized pre-processing defense (RAND-Pre) [61], Randomized post-processing defense (RAND-Post) [13], and Adversarial Training based TRADES [87]. Blacklight has recently proposed to mitigate query-based black-box attacks by utilizing the similarity among queries. It has been shown to detect 100% adversarial examples generated in multiple attacks. RAND-Pre and RAND-Post respectively add noise to the inputs and prediction logits to obfuscate the gradient estimation or local search. TRADES has demonstrated SOTA robustness performance against adversarial attacks by training on adversarial examples.

**Metrics.** We use the below metrics to evaluate all compared attacks.

- **Model Accuracy:** the model accuracy under attack and defense.
- **Number of RPQ (# RPQ):** the number of the randomized parallel query for certifiable attack.
- **Number of Query (# Q):** the total number of queries for empirical attack. For our method, it is equal to Monte Carlo Sampling Number  $\times$  # RPQ + additional queries for sampling from the *Adversarial Distribution*.

- **Certified Accuracy@p:** the certified accuracy at the ASP Threshold  $p$ . It is the percentage of the testing samples that have the certified ASP at least  $p$ , e.g., a 95% certified accuracy with ASP Threshold  $p = 90\%$  means the adversary can guarantee to have 90% probability to attack successfully for 95% testing samples.
- **$\ell_2$  Perturbation Size (Dist.  $\ell_2$ ):**  $\ell_2$  distance between the adversarial example  $x_{adv}$  and the clean input  $x$ , i.e.,  $\|x_{adv} - x\|_2$ .
- **$\ell_2$  Mean Distance (Mean Dist.  $\ell_2$ ):**  $\ell_2$  distance between the mean  $x'$  of *Adversarial Distribution* and clean input  $x$ , i.e.,  $\|x' - x\|_2$ .
- **Detection Success Rate (Det. Rate):** the detection success rate of Blacklight detection.
- **Average # Queries for Detection (# Q to Det.):** the average number of queries before Blacklight detects an AE.
- **Detection Coverage (Det. Cov.):** the percent of queries in an attack's query sequence that Blacklight identified as attack queries.

**Parameters Settings.** There exist many parameters that may affect the performance of our certifiable attack. For instance, the Monte Carlo sampling number, the attack success probability  $p$ , and the family of the adversarial distribution and its parameters. If not specified, we set Monte Carlo sampling number to be 50,  $p = 10\%$ , and use Gaussian distribution with variance  $\sigma = 0.025$ . We will also study the impact of these parameters in Section 5.3. All the parameter details are summarized in Table 12 in Appendix D.1.

**Experimental Environment.** We implemented a PyTorch library<sup>2</sup> including 16 black-box attacks, 4 defenses, 6 datasets, and 9 models by integrating several open-source libraries<sup>3</sup>. The experiments were run on a server with AMD EPYC Genoa 9354 CPUs (32 Core, 3.3GHz), and NVIDIA H100 Hopper GPUs (80GB each).

## 5.2 Verifying the Adversarial Distribution

We first assess the ASP of the crafted *Adversarial Distribution*. Specifically, given an ASP Threshold  $p$  and the certified *Adversarial Distribution*  $\varphi(x', \kappa)$ , we randomly sample 1,000 examples  $x_{adv} \sim \varphi(x', \kappa)$ , and query the model. We visualize the query results for 4 certified *Adversarial Distributions* with different  $p$  using 2D t-SNE<sup>4</sup> [77]. We also report the provable lower bound of ASP  $p_{adv}$  and the empirical ASP in Figure 5. It validates that the sampled AEs ensure the minimum ASP via the *Adversarial Distribution*, and the *Adversarial Distribution* lies on the decision boundary.

## 5.3 Attack Performance against SOTA Defenses

In this section, we evaluate our certifiable attack and empirical attacks against the 4 studied SOTA defenses.

**5.3.1 Attack Performance under Blacklight Detection [47].** We use the default setting from [47] with a threshold of 25. The results are presented in Table 3 and Tables 13-20 in Appendix D. We have the following key observations: 1) Our certifiable attack consistently circumvents Blacklight with 0% detection success rate, and 0% detection coverage on all settings, which means all the queries from our attack are not detected. Oppositely, existing black-box attacks suffer from Blacklight with 100% detection success rate for most

<sup>2</sup>All the code will be open-sourced upon paper acceptance.

<sup>3</sup>BlackboxBench, pytorch image classification, Blacklight, SparseEvo, and TRADES

<sup>4</sup>t-SNE reduces the prediction logits of the random samples to 2-dimension.



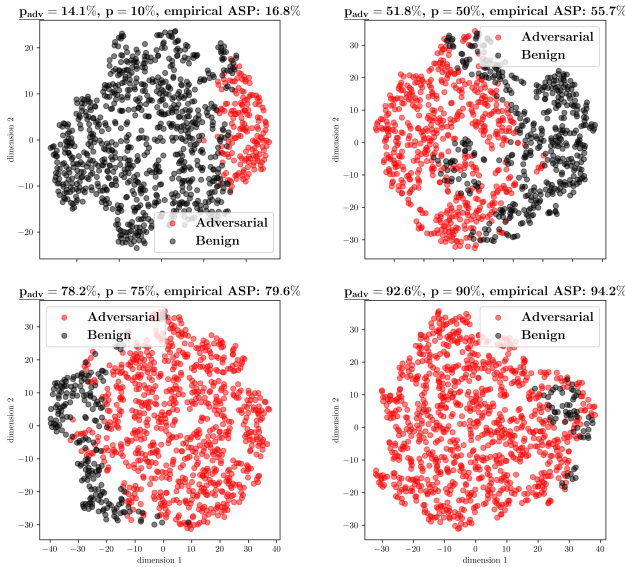


Figure 5: t-SNE Visualization of Adversarial Example Sampling from the *Adversarial Distribution*.

Table 3: Attack performance under Blacklight detection on ResNet and ImageNet (Clean Accuracy: 67.9%)

Attack	Query Type	Pert. Type	Det. Rate %	# Q to Det.	Det. Cov. %	Model Acc.	# Q	Dist. $\ell_2$
Bandit	Score	$\ell_\infty$	100.0	1.0	64.2	1.9	25	25.42
NES	Score	$\ell_\infty$	100.0	10.3	17.3	7.0	337	8.28
Parsimonious	Score	$\ell_\infty$	100.0	2.0	96.7	3.8	282	25.24
Sign	Score	$\ell_\infty$	100.0	2.0	91.5	0.5	126	25.50
Square	Score	$\ell_\infty$	100.0	2.0	66.9	0.0	14	25.54
ZOSignSGD	Score	$\ell_\infty$	100.0	2.0	50.2	12.5	322	8.53
GeoDA	Label	$\ell_\infty$	100.0	1.0	88.9	5.1	151	17.99
HSJ	Label	$\ell_\infty$	100.0	7.3	94.9	35.6	212	9.82
Opt	Label	$\ell_\infty$	99.9	8.4	81.4	61.2	646	0.98
RayS	Label	$\ell_\infty$	100.0	4.4	83.5	4.2	260	29.63
SignFlip	Label	$\ell_\infty$	100.0	8.5	70.3	4.4	148	27.64
SignOPT	Label	$\ell_\infty$	99.9	8.4	69.8	55.9	570	1.32
Bandit	Score	$\ell_2$	100.0	1.0	99.5	1.7	431	9.60
NES	Score	$\ell_2$	100.0	10.2	32.8	61.2	571	0.45
Simple	Score	$\ell_2$	100.0	1.0	99.9	53.6	883	0.88
Square	Score	$\ell_2$	100.0	2.0	68.8	0.0	16	26.30
ZOSignSGD	Score	$\ell_2$	100.0	2.0	52.4	65.1	531	0.30
Boundary	Label	$\ell_2$	100.0	7.2	76.3	37.9	60	11.63
GeoDA	Label	$\ell_2$	100.0	1.0	89.3	3.9	181	19.14
HSJ	Label	$\ell_2$	100.0	7.3	93.4	11.4	255	22.21
Opt	Label	$\ell_2$	100.0	8.5	67.9	41.2	610	16.71
SignOPT	Label	$\ell_2$	99.9	8.4	62.9	36.7	485	17.54
PointWise	Label	Opt.	100.0	1.0	99.8	0.0	920	13.53
SparseEvo	Label	Opt.	100.0	1.0	99.9	0.0	1000	7.68
CA (sssp)	Label	Opt.	0.0	$\infty$	0.0	1.4	148	13.74
CA (bin search)	Label	Opt.	0.0	$\infty$	0.0	0.0	603	33.14

Table 4: Attack performance under RAND Pre-processing Defense on ResNet and ImageNet (Clean Accuracy: 67.0%)

Attack	Query Type	Perturbation Type	# Query	Model Acc.	Dist. $\ell_2$
Bandit	Score	$\ell_\infty$	10	6.7	25.26
NES	Score	$\ell_\infty$	428	49.8	10.26
Parsimonious	Score	$\ell_\infty$	243	62.7	25.12
Sign	Score	$\ell_\infty$	116	40.6	25.20
Square	Score	$\ell_\infty$	27	10.4	24.96
ZOSignSGD	Score	$\ell_\infty$	428	49.4	10.36
GeoDA	Label	$\ell_\infty$	150	40.0	18.08
HSJ	Label	$\ell_\infty$	232	58.5	8.76
Opt	Label	$\ell_\infty$	905	69.4	0.44
RayS	Label	$\ell_\infty$	235	47.9	28.14
SignFlip	Label	$\ell_\infty$	46	52.8	13.06
SignOPT	Label	$\ell_\infty$	394	59.1	0.39
Bandit	Score	$\ell_2$	583	58.2	12.99
NES	Score	$\ell_2$	341	66.8	0.43
Simple	Score	$\ell_2$	258	67.2	0.10
Square	Score	$\ell_2$	18	13.6	25.96
ZOSignSGD	Score	$\ell_2$	249	67.3	0.28
Boundary	Label	$\ell_2$	38	49.2	15.12
GeoDA	Label	$\ell_2$	149	47.4	17.70
HSJ	Label	$\ell_2$	225	55.7	14.30
Opt	Label	$\ell_2$	1000	58.2	12.28
SignOPT	Label	$\ell_2$	406	52.2	15.41
PointWise	Label	Optimized	942	54.6	16.90
SparseEvo	Label	Optimized	1000	61.7	11.33
CA (sssp)	Label	Optimized	154	1.7	13.98
CA (bin search)	Label	Optimized	603	0.0	32.16

of the attacks on all datasets and models (the most resilient attack achieves 86.5% detection success rate on CIFAR100 and VGG16 in Table 17 in Appendix D). 2) With the strong ability to bypass the detection, our certifiable attack still maintains top attack performance on all the datasets and models such that the model accuracy can be attacked to 0% with moderate  $\ell_2$  perturbation size and few queries. The high attack accuracy and low detection rate of certifiable attacks stem from the randomness of *Adversarial Distribution* and the guarantee of the attack success probability.

**5.3.2 Attack Performance under RAND-Pre [61].** We follow [61] to inject the Gaussian noise with standard deviation 0.02 to the query (in the input space). The experimental results are presented in Table 4 and Tables 21-28 in Appendix D. Based on a comprehensive analysis of all results, it is evident that the RAND-Pre consistently reduces the attack success rate of existing black-box attacks. Specifically, the defense reduces the average attack success rate of empirical black-box attacks from 92% to 30% on CIFAR10, from 95% to 29% on CIFAR100, and from 69% to 25% on ImageNet, respectively. However, our attack still achieves the average attack success rate of 93%, 99%, and 99% respectively on the three datasets under RAND-Pre. Further, we highlight that, with RAND-Pre applied across all datasets and models, the average  $\ell_2$  perturbation size and number of queries in our certifiable attack *decrease* by 4.2% and 2.1%, respectively. This intriguing observation matches our findings in Section 5.4.1 where a larger variance leads to smaller  $\ell_2$  mean distance and # RPQ in the certifiable attack. This is because the Gaussian noise injected by the defense (e.g.,  $\epsilon_1 \sim \mathcal{N}(0, v)$ ) is added to the adversary’s noise (e.g.,  $\epsilon_2 \sim \mathcal{N}(0, u)$ ), leading to a larger variance  $v + u$  and hence further enhancing our attack.

**Table 5: Attack performance under RAND Post-processing Defense on ResNet and ImageNet (Clean Accuracy: 68.0%)**

Attack	Query Type	Perturbation Type	# Query	Model Acc.	Dist. $\ell_2$
Bandit	Score	$\ell_\infty$	17	2.7	25.51
NES	Score	$\ell_\infty$	378	18.6	9.53
Parsimonious	Score	$\ell_\infty$	253	47.9	25.46
Sign	Score	$\ell_\infty$	124	8.1	25.81
Square	Score	$\ell_\infty$	18	0.8	25.44
ZOSignSGD	Score	$\ell_\infty$	376	21.4	9.71
GeoDA	Label	$\ell_\infty$	143	38.6	17.62
HSJ	Label	$\ell_\infty$	212	52.7	8.82
Opt	Label	$\ell_\infty$	1000	65.3	0.67
RayS	Label	$\ell_\infty$	243	43.9	28.09
SignFlip	Label	$\ell_\infty$	86	47.2	15.44
SignOPT	Label	$\ell_\infty$	412	63.6	0.64
Bandit	Score	$\ell_2$	596	6.0	13.96
NES	Score	$\ell_2$	344	59.7	0.44
Simple	Score	$\ell_2$	241	58.9	0.10
Square	Score	$\ell_2$	23	0.4	26.46
ZOSignSGD	Score	$\ell_2$	275	61.4	0.29
Boundary	Label	$\ell_2$	24	48.0	12.64
GeoDA	Label	$\ell_2$	146	40.6	16.89
HSJ	Label	$\ell_2$	238	49.5	14.59
Opt	Label	$\ell_2$	1000	53.9	12.62
SignOPT	Label	$\ell_2$	411	46.3	15.96
PointWise	Label	Optimized	969	55.1	16.01
SparseEvo	Label	Optimized	1000	66.7	9.10
<b>CA (sssp)</b>	Label	Optimized	147	1.4	13.70
<b>CA (bin search)</b>	Label	Optimized	603	0.0	32.67

5.3.3 *Attack Performance under RAND-Post [13].* We follow [13] to inject the Gaussian noise with standard deviation 0.2 to the output logits of each query (applied to both hard label-based and score-based attacks). The experimental results are presented in Table 5, and Tables 29-36. Similarly, we find that RAND-Post can strongly degrade the average attack success rate of hard label-based empirical attacks from 84% to 41% on CIFAR10, from 89% to 45% on CIFAR100, and from 60% to 24% on ImageNet, respectively. On the other hand, it moderately degrades the average attack success rate of score-based empirical attacks from 100% to 91% on CIFAR10, from 100% to 95% on CIFAR100, and from 72% to 62% on ImageNet. The discrepancy between label-based and score-based empirical attacks may stem from variations in the richness and smoothness of the query information. The loss value (score), providing a smoother evaluation, is less susceptible to noise interference and discloses finer-grained details. In contrast, labels are more likely to be impacted by injected noise, resulting in more randomized query outcomes. However, our hard-label certifiable attack shows strong resilience against RAND-Post, by maintaining the average attack success rate at 93%, 99%, and 99% on CIFAR10, CIFAR100, and ImageNet, respectively. This advantage over empirical attacks, particularly the label-based ones, originates from the Randomized Parallel Querying—It precisely assesses query results with a lower bound of the ASP.

5.3.4 *Attack Performance under TRADES [87].* We consider both  $\ell_\infty$  and  $\ell_2$  perturbations to generate adversarial examples, and TRADES respectively uses  $\ell_2$  or  $\ell_\infty$  adversarial examples for adversarial training. We set the perturbation size to be  $\ell_\infty = 0.1$  and  $\ell_2 = 5$ , following [87]. We then evaluate all attacks against TRADES. The results on

**Table 6: Attack performance under TRADES Adversarial Training on ResNet and CIFAR10**

Defense	Attack	Query Type	Pert. Type	# Query	Model Acc.	Dist. $\ell_2$
$\ell_\infty$ Adversarial Training (Clean Accuracy: 80.9%)	Bandit	Score	$\ell_\infty$	1601	10.2	4.32
	NES	Score	$\ell_\infty$	1474	27.4	2.27
	Parsimonious	Score	$\ell_\infty$	630	5.3	4.35
	Sign	Score	$\ell_\infty$	439	4.4	4.37
	Square	Score	$\ell_\infty$	854	5.7	4.39
	ZOSignSGD	Score	$\ell_\infty$	1196	37.0	2.21
	GeoDA	Label	$\ell_\infty$	1358	41.9	1.99
	HSJ	Label	$\ell_\infty$	2149	36.5	1.92
	Opt	Label	$\ell_\infty$	1871	73.0	0.19
	RayS	Label	$\ell_\infty$	721	7.3	4.29
	SignFlip	Label	$\ell_\infty$	2240	24.4	3.36
	SignOPT	Label	$\ell_\infty$	832	69.3	0.15
	PointWise	Label	Opt.	3460	9.3	4.38
	SparseEvo	Label	Opt.	8691	9.1	5.10
	<b>CA (sssp)</b>	Label	Opt.	548	21.2	4.29
	<b>CA (bin search)</b>	Label	Opt.	412	9.8	6.31
$\ell_2$ Adversarial Training (Clean Accuracy: 59.2%)	Bandit	Score	$\ell_2$	860	1.5	2.44
	NES	Score	$\ell_2$	3535	9.5	0.99
	Simple	Score	$\ell_2$	4062	2.1	1.29
	Square	Score	$\ell_2$	991	4.6	2.95
	ZOSignSGD	Score	$\ell_2$	3505	15.1	0.77
	Boundary	Label	$\ell_2$	771	40.7	1.19
	GeoDA	Label	$\ell_2$	1506	14.3	2.85
	HSJ	Label	$\ell_2$	1332	5.1	3.53
	Opt	Label	$\ell_2$	2890	41.6	2.39
	SignOPT	Label	$\ell_2$	1766	33.6	2.76
	PointWise	Label	Opt.	4845	0.6	5.36
	SparseEvo	Label	Opt.	9697	0.4	6.03
	<b>CA (sssp)</b>	Label	Opt.	809	20.4	6.06
	<b>CA (bin search)</b>	Label	Opt.	461	0.0	8.18

CIFAR10 are presented in Table 6<sup>5</sup>. We observe our attack requires much less query number than the empirical attacks. Also, our attack can achieve 100% attack success rate (with the binary search localization), but at the cost of a relatively larger perturbation size.

## 5.4 Ablation Study

In this section, we explore in-depth our certifiable attack—we study its performance with varying noise variances, ASP thresholds, localization and shifting methods, and noise PDFs. We mainly show results on the image datasets and defer results on the audio dataset to Appendix D, where similar performance can be observed.

5.4.1 *Attack Performance on Different Noise Variances.* Table 7 shows the performance of our attack with varying noise variances used in  $\varphi$ . We have the following key observations: 1) As the variance increases, the  $\ell_2$  perturbation size increases, since larger variance results in larger noise. 2) The  $\ell_2$  mean distance tends to decrease as the variance increases. This could be because that larger variance covers a larger decision space, and without moving the mean far away from the clean input, we can easily find a large portion of adversarial samples under the distribution with a large variance. 3) As the variance increases, the number of RPQ decreases. This is because the larger variance usually leads to a larger shifting step. It takes fewer iterations to move to the decision boundary when the variance increases. 4) Finally, a larger certified accuracy means that it is easier to determine the *Adversarial Distribution*.

<sup>5</sup>It is computationally-intensive and time-consuming to train TRADES on CIFAR100 and ImageNet

**Table 7: Attack performance of our certifiable attack with varying Gaussian noise variances  $\sigma$  ( $p = 90\%$ )**

	$\sigma$	Dist. $\ell_2$	Mean Dist. $\ell_2$	# RPQ	Certified Acc.
CIFAR10	0.10	7.39	3.96	18.34	94.17%
	0.25	12.95	2.34	14.35	91.21%
	0.50	19.41	0.43	11.38	90.00%
ImageNet	0.10	41.80	16.78	32.55	99.80%
	0.25	87.47	16.78	17.02	99.60%
	0.50	135.47	2.27	8.31	100.00%

**Table 8: Attack performance of our certifiable attack with varying  $p$  under the Gaussian variance  $\sigma = 0.25$** 

	$p$	Dist. $\ell_2$	Mean Dist. $\ell_2$	# RPQ	Certified Acc.
CIFAR10	50%	12.65	1.63	9.34	97.17%
	60%	12.72	1.86	11.09	95.85%
	70%	12.80	2.05	11.94	94.72%
	80%	12.87	2.18	12.37	93.17%
	90%	12.95	2.34	14.35	91.21%
	95%	13.09	2.65	15.93	90.37%
ImageNet	50%	85.88	9.89	12.85	100.00%
	60%	86.20	11.30	13.63	100.00%
	70%	86.45	12.64	14.33	100.00%
	80%	87.03	14.64	16.02	100.00%
	90%	87.47	16.78	17.02	99.60%
	95%	88.42	19.98	19.81	100.00%

**Table 9: Attack performance of our certifiable attack on different localization/refinement algorithms ( $\sigma = 0.25$ ,  $p = 90\%$ )**

Localization	Refinement	Dist. $\ell_2$	Mean Dist. $\ell_2$	# RPQ	Cert. Acc.
sssp	none	11.46	1.35	2.30	92.54
binary search	none	11.29	0.34	9.07	92.54
random	geo.	11.80	1.73	67.53	92.54
sssp	geo.	11.20	0.49	3.70	91.54
binary search	geo.	11.28	0.27	10.08	92.53

The results on CIFAR10 show that it is easier to find a small area of adversarial examples than a large area of adversarial examples. On ImageNet, we observe nearly 100% certified accuracy, which means it is relatively easy to find the adversarial examples on datasets with a large number of classes (since 999 out of 1,000 classes in ImageNet are all false classes) or with high feature dimension.

**5.4.2 Attack Performance on Different ASP Thresholds.** We study the relationship between the performance of our attack and the ASP threshold, and Table 8 shows the results. As  $p$  increases, so do the  $\ell_2$  perturbation size, the  $\ell_2$  mean distance, and the number of RPQ. On one hand, a larger  $p$  means it requires more adversarial examples to fall into the false classes. When the noise variance is fixed, the mean of the *Adversarial Distribution* should be further away from the decision boundary to allow more adversarial examples to fall into the false classes. On the other hand, the smaller  $p$  results in a larger shifting distance, which depends on the gap between  $p$  and  $p_{adv}$  (see the Gaussian-case of Theorem 1 in Appendix A.2). With a larger shifting distance, the required number of RPQ can be fewer. We also observe that a smaller  $p$  results in a higher certified accuracy on CIFAR10, since a smaller  $p$  allows more “failed” adversarial examples. On ImageNet, the certified accuracy is consistently ~

100%, no matter  $p$ ’s value. This might still due to that it is much easier to find adversarial examples with a much larger number of classes.

**5.4.3 Attack Performance on Different Localization/Refinement Algorithms.** In this experiment, we evaluate the attack performance under our proposed localization and refinement methods. Specifically, we compare our proposed Smoothed SSP and binary-search localization methods with the random localization baseline; and compare our proposed geometric shifting method with a no-shifting baseline. Experimental results are shown in Table 9. We observe that the combination of the localization and refinement methods yields the smallest perturbation size, i.e., the smallest Dist.  $\ell_2$  and Mean Dist.  $\ell_2$ . This demonstrates that they are both effective in improving the imperceptibility of adversarial examples.

**5.4.4 Attack Performance on Different Noise Distributions.** Our attack can use any continuous noise distribution to craft the *Adversarial Distribution*. Besides the Gaussian noise distribution, in this experiment, we also evaluate the performance of our certifiable attack using other noise distributions including the Cauchy distribution, Hyperbolic Secant distribution, and general normal distributions. Note that we adjust the parameters in these distributions to ensure consistent variances for a fair comparison.

The results are presented in Table 10, and the noise distributions are plotted in Figure 9 in Appendix. On both datasets, we observe the  $\ell_2$  perturbation size is decreasing while the  $\ell_2$  mean distance is increasing as the PDF of the noise distribution is more centralized. This result may share a similar nature with results in Table 7—when the adversarial samples are more widely distributed, they tend to fall into an adversarial class (the majority of all classes). It is hard to determine which distribution is better since there is a trade-off between the perturbation size and the number of RPQ.

## 5.5 Defending against Our Certifiable Attack

In this subsection, we discuss potential defenses and mitigation strategies against our attacks.

**Noise Detection based Defenses:** Our certifiable attack injects noise into the adversarial examples. Here, we suppose the adversary is aware of the noise injection and designs a detection method by training a binary classifier to distinguish the noise-injected inputs and clean inputs. Specifically, the defender (i.e., model owner) uses ResNet110 (as powerful as the target model) to train a noise detector to distinguish the inputs with and without noise. The experimental results show the noise detection rate can be as high as 99% with the noise variance  $\sigma = 0.5$ , which means this detector can be used as a strong defense against our certifiable attacks with a larger noise. However, this defense does not work when the noise scale is smaller (i.e.,  $\sigma = 0.025$ ), where the detection rate is less than 1%. Especially, the adversary may design a novel method to hide this noise in the image texture, e.g., using the diffusion model for denoising, which may circumvent the detection.

**White-Box Adaptive Defenses against Our Attack:** We assume the model owner knows the noise distribution used by our attack

**Table 10: Attack performance of our certifiable attack with different noise distributions**

	Distribution	Density	Parameter	$\sqrt{\ \epsilon\ ^2/d}$	Dist. $\ell_2$	Mean Dist. $\ell_2$	# RPQ	Certified Acc.
CIFAR10	Gaussian	$\propto e^{- z/a ^2}$	$a = 0.25$	0.25	12.95	2.34	14.35	91.21%
	Cauchy	$\propto \frac{a^2}{z^2+a^2}$	$a = 0.01969$	0.25	7.82	4.87	32.77	94.12%
	Hyperbolic Secant	$\propto \text{sech}( z/a )$	$a = 0.1592$	0.25	12.51	2.43	14.59	91.67%
	General Normal ( $b = 1.5$ )	$\propto e^{- z/a ^b}$	$a = 0.2909, b = 1.5$	0.25	12.74	2.37	14.15	91.39%
	General Normal ( $b = 3.0$ )	$\propto e^{- z/a ^b}$	$a = 0.4092, b = 3$	0.25	13.16	2.38	14.15	91.25%
ImageNet	Gaussian	$\propto e^{- z/a ^2}$	$a = 0.25$	0.25	87.47	16.78	17.02	99.60%
	Cauchy	$\propto \frac{a^2}{z^2+a^2}$	$a = 0.01969$	0.25	46.18	23.94	59.94	99.60%
	Hyperbolic Secant	$\propto \text{sech}( z/a )$	$a = 0.1592$	0.25	85.57	21.29	20.89	99.80%
	General Normal ( $b = 1.5$ )	$\propto e^{- z/a ^b}$	$a = 0.2909, b = 1.5$	0.25	86.69	19.05	17.58	99.80%
	General Normal ( $b = 3.0$ )	$\propto e^{- z/a ^b}$	$a = 0.4092, b = 3$	0.25	88.51	15.58	14.99	100.00%

**Table 11: White-box adaptive defense against our attack ( $\sigma = 0.25, p = 90\%$ ) on CIFAR10**

Defense Para.	Dist. $\ell_2$	Mean Dist. $\ell_2$	# RPQ	Cert. Acc.
$\sigma_d = 0.10$	9.99	7.73	34.11	87.51%
$\sigma_d = 0.25$	15.40	10.21	29.80	88.31%
$\sigma_d = 0.50$	20.46	8.11	26.52	86.56%

and performs a “white-box” defense. Particularly, it applies a denoiser to eliminate the injected noise, so that the adversarial examples can be restored to clean inputs. The denoiser can be deployed as a pre-processing module and is pre-trained by the model owner.

Specifically, we use a U-Net structure [64] as the denoiser and denote it as  $\mathcal{D}$ . Then, the loss function for the training is

$$\mathbb{E}_{\epsilon \sim \mathcal{N}(0, \sigma_d)} [\|\mathcal{D}(x + \epsilon) - x\|_2 + \|f(\mathcal{D}(x + \epsilon)) - f(x)\|_2] \quad (8)$$

Taking Gaussian noise as an example (e.g., the model owner knows the Gaussian variance  $\sigma = 0.25$  used in the certifiable attack), we train the denoiser to eliminate Gaussian noise with  $\sigma = 0.25$  while evaluating the certifiable attack with Gaussian noise generated by different  $\sigma$ . Table 11 shows the results. We can observe that this defense can significantly degrade the performance of a certifiable attack. Notably, by choosing the same variance  $\sigma$  as the adversary, the adaptive defense can increase the Mean Dist.  $\ell_2$  significantly. However, the certified accuracy is still near 90%.

## 6 RELATED WORK

**Adversarial Attack.** It aims to mislead learnt ML models by perturbing testing data with imperceptible perturbations. It can be divided into white-box attacks [12, 30, 53, 56, 80] and black-box attacks [2, 5, 7, 7, 8, 14, 16, 16, 19, 25, 26, 31, 38, 39, 48, 58, 59, 70], per the access that the adversary holds. White-box attacks have full access to the model parameters, and can leverage the gradient of the loss function w.r.t. the inputs to guide the adversarial example generation. Instead, black-box attacks only know the outputs (in the form of prediction scores or labels) of a target model via sending queries. It is widely believed that black-box attack is more practical in real-world scenarios [6, 14, 59]. Therefore, we focus on the black-box attacks in this paper.

**Black-Box Attack.** Existing black-box attack methods can be classified into three types: gradient estimation based [5, 16, 19, 26, 39], surrogate models based [25, 58, 59, 70], or local search based algorithms [2, 7, 8, 31, 48]. Gradient estimation based attack is mainly based on

zero-order estimation since the true gradient is unknown [16]. Surrogate model based methods first perform white-box attacks on an offline surrogate model to generate adversarial examples, and then use these generated adversarial examples to test the target model. The attack performance largely depends on the transferability of such generated adversarial examples. Local search based methods craft adversarial examples by searching the effective perturbation direction. For example, Boundary Attack [7] traverses the decision boundary to craft the *least imperceptible* perturbations.

All existing black-box attacks rely on querying the target model until finding a successful adversarial example or reaching the maximum number of queries. However, none of them can ensure the success rate of the adversarial examples that have not been queried. Further, they are shown to be easily detected/removed via adversarial detection and randomized pre/post-processing based defenses.

**Empirical Defense.** It defends against adversarial attacks without guarantees. Empirical defenses against white-box attacks can be roughly categorized into four classes. Gradient-masking defenses [24, 60, 81] modify the model inference process to obstacle the gradient computation. Input-transformation defenses [9, 32, 36, 49, 67, 72] use pre-processing methods to transform the inputs so that the malicious effects caused by the perturbations can be reduced. Detection-based defenses [41, 52, 54, 65, 74] identify features that expect to separate adversarial examples and clean examples, and train a binary classifier to detect adversarial examples. These three types of defenses show certain effectiveness when they target specific known attacks, but can be broken by adaptive attacks [4]. Lastly, adversarial training-based defenses [53, 69, 75, 76] have achieved the SOTA performance against adaptive attacks. The main idea is to augment training data with “adversarial examples”, but they are reassigned the correct label. As to defend against *black-box* attacks, RAND-Post [13], RAND-Pre [61], Adversarial Training based TRADES [53], and Blacklight [47] are the SOTA in each category. Thus, we evaluated our certifiable attack under these defenses.

**Certified Defense.** Certified defense [3, 28, 42, 79] was proposed to guarantee constant classification prediction on a set of adversarial examples. Recently, randomized smoothing (RS) [22] has achieved great success in the certified defense since it is the first method that can certify arbitrary classifiers of any scale. Specifically, RS can guarantee the prediction if the perturbation is bounded by a distance in  $\ell_p$ -norm, i.e., certified radius [22, 73, 85]. RS adds noise

from a fixed distribution (e.g., Gaussian) to the inputs and uses hypothesis testing to quantify the prediction probability over the noise distribution. Then the constraint on the perturbations (usually a  $\ell_p$  norm constraint) for ensuring the consistent prediction is theoretically derived. This method is widely used in certified defense to ensure consistent and correct prediction under attack. However, in this paper, we propose to leverage this method to ensure consistent and wrong prediction on the *Adversarial Distribution*, resulting in a reliable and strong certifiable attack.

## 7 CONCLUSION

Certifiable attack lays a novel direction for adversarial attacks, enabling the transition from deterministic to probabilistic adversarial attacks. Compared with empirical black-box attacks, certifiable attacks share significant benefits including breaking SOTA strong detection and randomized defense, revealing consistent and severe robustness vulnerability of models, and guaranteeing the minimum ASP for numerous unique AEs without verifying via the query.

## REFERENCES

- [1] Abdullah Al-Dujaili and Una-May O'Reilly. Sign bits are all you need for black-box attacks. In *8th International Conference on Learning Representations, ICLR 2020, Addis Ababa, Ethiopia, April 26–30, 2020*. OpenReview.net, 2020.
- [2] Maksym Andriushchenko, Francesco Croce, Nicolas Flammarion, and Matthias Hein. Square attack: A query-efficient black-box adversarial attack via random search. In Andrea Vedaldi, Horst Bischof, Thomas Brox, and Jan-Michael Frahm, editors, *ECCV*, volume 12368 of *Lecture Notes in Computer Science*, pages 484–501. Springer, 2020.
- [3] Cem Anil, James Lucas, and Roger B. Grosse. Sorting out lipschitz function approximation. In *ICML*, volume 97, pages 291–301. PMLR, 2019.
- [4] Anish Athalye, Nicholas Carlini, and David Wagner. Obfuscated gradients give a false sense of security: Circumventing defenses to adversarial examples. In *International conference on machine learning*, pages 274–283. PMLR, 2018.
- [5] Arjun Nitin Bhagoji, Warren He, Bo Li, and Dawn Song. Practical black-box attacks on deep neural networks using efficient query mechanisms. In *ECCV*. Springer, 2018.
- [6] Siddhant Bhambri, Sumanyu Muku, Avinash Tulasi, and Arun Balaji Buduru. A survey of black-box adversarial attacks on computer vision models. *arXiv preprint arXiv:1912.01667*, 2019.
- [7] Wieland Brendel, Jonas Rauber, and Matthias Bethge. Decision-based adversarial attacks: Reliable attacks against black-box machine learning models. In *ICLR*. OpenReview.net, 2018.
- [8] Thomas Brunner, Frederik Diehl, Michael Truong-Le, and Alois C. Knoll. Guessing smart: Biased sampling for efficient black-box adversarial attacks. In *ICCV*, pages 4957–4965. IEEE, 2019.
- [9] Jacob Buckman, Aurko Roy, Colin Raffel, and Ian J. Goodfellow. Thermometer encoding: One hot way to resist adversarial examples. In *ICLR*. OpenReview.net, 2018.
- [10] Joseph P Campbell. Speaker recognition: A tutorial. *Proceedings of the IEEE*, 85(9):1437–1462, 1997.
- [11] Nicholas Carlini, Florian Tramèr, Krishnamurthy Dj Dvijotham, Leslie Rice, Mingjie Sun, and J Zico Kolter. (certified!!) adversarial robustness for free! *arXiv preprint arXiv:2206.10550*, 2022.
- [12] Nicholas Carlini and David A. Wagner. Towards evaluating the robustness of neural networks. In *2017 IEEE Symposium on Security and Privacy*, pages 39–57. IEEE Computer Society, 2017.
- [13] Varun Chandrasekaran, Kamalika Chaudhuri, Irene Giacomelli, Somesh Jha, and Songbai Yan. Exploring connections between active learning and model extraction. In Srdjan Capkun and Franziska Roesner, editors, *29th USENIX Security Symposium, USENIX Security 2020, August 12–14, 2020*, pages 1309–1326. USENIX Association, 2020.
- [14] Jianbo Chen, Michael I. Jordan, and Martin J. Wainwright. Hopskipjumpattack: A query-efficient decision-based attack. In *IEEE Symposium on Security and Privacy*, pages 1277–1294. IEEE, 2020.
- [15] Jinghui Chen and Quanquan Gu. Rays: A ray searching method for hard-label adversarial attack. In Rajesh Gupta, Yan Liu, Jiliang Tang, and B. Aditya Prakash, editors, *KDD '20: The 26th ACM SIGKDD Conference on Knowledge Discovery and Data Mining, Virtual Event, CA, USA, August 23–27, 2020*, pages 1739–1747. ACM, 2020.
- [16] Pin-Yu Chen, Huan Zhang, Yash Sharma, Jinfeng Yi, and Cho-Jui Hsieh. ZOO: zeroth order optimization based black-box attacks to deep neural networks without training substitute models. In Bhavani Thuraisingham, Battista Biggio, David Mandell Freeman, Brad Miller, and Arunesh Sinha, editors, *AISec@CCS*, pages 15–26. ACM, 2017.
- [17] Sizhe Chen, Zehao Huang, Qinghua Tao, Yingwen Wu, Cihang Xie, and Xiaolin Huang. Adversarial attack on attackers: Post-process to mitigate black-box score-based query attacks. *Advances in Neural Information Processing Systems*, 35:14929–14943, 2022.
- [18] Weilun Chen, Zhaoxiang Zhang, Xiaolin Hu, and Baoyuan Wu. Boosting decision-based black-box adversarial attacks with random sign flip. In Andrea Vedaldi, Horst Bischof, Thomas Brox, and Jan-Michael Frahm, editors, *Computer Vision - ECCV 2020 - 16th European Conference, Glasgow, UK, August 23–28, 2020, Proceedings, Part XV*, volume 12360 of *Lecture Notes in Computer Science*, pages 276–293. Springer, 2020.
- [19] Minhao Cheng, Thong Le, Pin-Yu Chen, Huan Zhang, Jinfeng Yi, and Cho-Jui Hsieh. Query-efficient hard-label black-box attack: An optimization-based approach. In *ICLR*. OpenReview.net, 2019.
- [20] Minhao Cheng, Simranjit Singh, Patrick H. Chen, Pin-Yu Chen, Sijia Liu, and Cho-Jui Hsieh. Sign-opt: A query-efficient hard-label adversarial attack. In *8th International Conference on Learning Representations, ICLR 2020, Addis Ababa, Ethiopia, April 26–30, 2020*. OpenReview.net, 2020.
- [21] J. S. Chung, A. Nagrani, and A. Zisserman. Voxceleb2: Deep speaker recognition. In *INTERSPEECH*, 2018.
- [22] Jeremy M. Cohen, Elan Rosenfeld, and J. Zico Kolter. Certified adversarial robustness via randomized smoothing. In Kamalika Chaudhuri and Ruslan Salakhutdinov, editors, *ICML*, volume 97 of *Proceedings of Machine Learning Research*, pages

- 1310–1320. PMLR, 2019.
- [23] Brecht Desplanques, Jenthe Thienpondt, and Kris Demuynck. Ecapa-tdnn: Emphasized channel attention, propagation and aggregation in tdnn based speaker verification. 2020.
- [24] Guneet S. Dhillon, Kamyar Azizzadenesheli, Zachary C. Lipton, Jeremy Bernstein, Jean Kossaifi, Aran Khanna, and Animashree Anandkumar. Stochastic activation pruning for robust adversarial defense. In *ICLR*. OpenReview.net, 2018.
- [25] Yinpeng Dong, Tianyu Pang, Hang Su, and Jun Zhu. Evading defenses to transferable adversarial examples by translation-invariant attacks. In *IEEE Conference on Computer Vision and Pattern Recognition, CVPR 2019*, pages 4312–4321. Computer Vision Foundation / IEEE, 2019.
- [26] Yali Du, Meng Fang, Jinfeng Yi, Jun Cheng, and Dacheng Tao. Towards query efficient black-box attacks: An input-free perspective. In Sadia Afroz, Battista Biggio, Yuval Elovici, David Freeman, and Asaf Shabtai, editors, *Proceedings of the 11th ACM Workshop on Artificial Intelligence and Security, CCS 2018*, pages 13–24. ACM, 2018.
- [27] Aryeh Dvoretzky, Jack Kiefer, and Jacob Wolfowitz. Asymptotic minimax character of the sample distribution function and of the classical multinomial estimator. *The Annals of Mathematical Statistics*, pages 642–669, 1956.
- [28] Matteo Fischetti and Jason Jo. Deep neural networks and mixed integer linear optimization. *Constraints An Int. J.*, 23(3):296–309, 2018.
- [29] Daniel Garcia-Romero, David Snyder, Gregory Sell, Alan McCree, Daniel Povey, and Sanjeev Khudanpur. x-vector dnn refinement with full-length recordings for speaker recognition. In *Interspeech*, pages 1493–1496, 2019.
- [30] Ian J. Goodfellow, Jonathon Shlens, and Christian Szegedy. Explaining and harnessing adversarial examples. In Yoshua Bengio and Yann LeCun, editors, *3rd International Conference on Learning Representations, ICLR 2015*, 2015.
- [31] Chuan Guo, Jacob R. Gardner, Yurong You, Andrew Gordon Wilson, and Kilian Q. Weinberger. Simple black-box adversarial attacks. In *ICML 2019*.
- [32] Chuan Guo, Mayank Rana, Moustapha Cissé, and Laurens van der Maaten. Countering adversarial images using input transformations. In *6th International Conference on Learning Representations, ICLR 2018*. OpenReview.net, 2018.
- [33] Kaiming He, Xiangyu Zhang, Shaoqing Ren, and Jian Sun. Deep residual learning for image recognition. In *Proceedings of the IEEE conference on computer vision and pattern recognition*, pages 770–778, 2016.
- [34] Zhezhi He, Adnan Siraj Rakin, and Deliang Fan. Parametric noise injection: Trainable randomness to improve deep neural network robustness against adversarial attack. In *Proceedings of the IEEE/CVF Conference on Computer Vision and Pattern Recognition*, pages 588–597, 2019.
- [35] Jonathan Ho, Ajay Jain, and Pieter Abbeel. Denoising diffusion probabilistic models. *Advances in neural information processing systems*, 33:6840–6851, 2020.
- [36] Hanbin Hong, Yuan Hong, and Yu Kong. An eye for an eye: Defending against gradient-based attacks with gradients. *arXiv preprint arXiv:2202.01117*, 2022.
- [37] Hanbin Hong, Binghui Wang, and Yuan Hong. Unicr: Universally approximated certified robustness via randomized smoothing. In *European Conference on Computer Vision*, pages 86–103. Springer, 2022.
- [38] Andrew Ilyas, Logan Engstrom, Anish Athalye, and Jessy Lin. Query-efficient black-box adversarial examples. *CoRR*, abs/1712.07113, 2017.
- [39] Andrew Ilyas, Logan Engstrom, Anish Athalye, and Jessy Lin. Black-box adversarial attacks with limited queries and information. In *Proceedings of the 35th International Conference on Machine Learning, ICML 2018*, Proceedings of Machine Learning Research. PMLR, 2018.
- [40] Andrew Ilyas, Logan Engstrom, and Aleksander Madry. Prior convictions: Black-box adversarial attacks with bandits and priors. In *7th International Conference on Learning Representations, ICLR 2019, New Orleans, LA, USA, May 6-9, 2019*. OpenReview.net, 2019.
- [41] Shubham Jain, Ana-Maria Cretu, and Yves-Alexandre de Montjoye. Adversarial detection avoidance attacks: Evaluating the robustness of perceptual hashing-based client-side scanning. In *31st USENIX Security Symposium (USENIX Security 22)*, pages 2317–2334, 2022.
- [42] Guy Katz, Clark W. Barrett, David L. Dill, Kyle Julian, and Mykel J. Kochenderfer. Reluplex: An efficient SMT solver for verifying deep neural networks. In *Computer Aided Verification - 29th International Conference, CAV 2017, Lecture Notes in Computer Science*, 2017.
- [43] Matěj Korvas, Ondřej Plátek, Ondřej Dušek, Lukáš Žilka, and Filip Jurčiček. Free English and Czech telephone speech corpus shared under the CC-BY-SA 3.0 license. In *(LREC 2014)*, 2014.
- [44] Alex Krizhevsky, Geoffrey Hinton, et al. Learning multiple layers of features from tiny images. 2009.
- [45] Alexey Kurakin, Ian J. Goodfellow, and Samy Bengio. Adversarial machine learning at scale. In *5th International Conference on Learning Representations, ICLR 2017*. OpenReview.net, 2017.
- [46] Mathias Lecuyer, Vaggelis Atlidakis, Roxana Geambasu, Daniel Hsu, and Suman Jana. Certified robustness to adversarial examples with differential privacy. In *2019 IEEE Symposium on Security and Privacy (SP)*, pages 656–672. IEEE, 2019.
- [47] Huiying Li, Shawn Shan, Emily Wenger, Jiayun Zhang, Haitao Zheng, and Ben Y. Zhao. Blacklight: Scalable defense for neural networks against query-based black-box attacks. In Kevin R. B. Butler and Kurt Thomas, editors, *31st USENIX Security Symposium, USENIX Security 2022, Boston, MA, USA, August 10-12, 2022*, pages 2117–2134. USENIX Association, 2022.
- [48] Yandong Li, Lijun Li, Liqiang Wang, Tong Zhang, and Boqing Gong. NATTACK: learning the distributions of adversarial examples for an improved black-box attack on deep neural networks. In Kamalika Chaudhuri and Ruslan Salakhutdinov, editors, *ICML 2019, Proceedings of Machine Learning Research*. PMLR, 2019.
- [49] Fangzhou Liao, Ming Liang, Yinpeng Dong, Tianyu Pang, Xiaolin Hu, and Jun Zhu. Defense against adversarial attacks using high-level representation guided denoiser. In *2018 IEEE Conference on Computer Vision and Pattern Recognition, CVPR 2018*, pages 1778–1787. Computer Vision Foundation / IEEE Computer Society, 2018.
- [50] Sijia Liu, Pin-Yu Chen, Xiangyi Chen, and Mingyi Hong. signsgd via zeroth-order oracle. In *7th International Conference on Learning Representations, ICLR 2019, New Orleans, LA, USA, May 6-9, 2019*. OpenReview.net, 2019.
- [51] Xuanqing Liu, Minhao Cheng, Huan Zhang, and Cho-Jui Hsieh. Towards robust neural networks via random self-ensemble. In *Proceedings of the european conference on computer vision (ECCV)*, pages 369–385, 2018.
- [52] Jiajun Lu, Theerarat Issaranon, and David A. Forsyth. Safetynet: Detecting and rejecting adversarial examples robustly. In *IEEE International Conference on Computer Vision, ICCV 2017*, pages 446–454. IEEE Computer Society, 2017.
- [53] Aleksander Madry, Aleksandar Makelov, Ludwig Schmidt, Dimitris Tsipras, and Adrian Vladu. Towards deep learning models resistant to adversarial attacks. In *6th International Conference on Learning Representations, ICLR 2018*. OpenReview.net, 2018.
- [54] Dongyu Meng and Hao Chen. Magnet: A two-pronged defense against adversarial examples. In Bhavani Thuraisingham, David Evans, Tal Malkin, and Dongyan Xu, editors, *Proceedings of the 2017 ACM SIGSAC Conference on Computer and Communications Security, CCS 2017*, pages 135–147. ACM, 2017.
- [55] Seungyong Moon, Gaon An, and Hyun Oh Song. Parsimonious black-box adversarial attacks via efficient combinatorial optimization. In Kamalika Chaudhuri and Ruslan Salakhutdinov, editors, *Proceedings of the 36th International Conference on Machine Learning, ICML 2019, 9-15 June 2019, Long Beach, California, USA*, volume 97 of *Proceedings of Machine Learning Research*, pages 4636–4645. PMLR, 2019.
- [56] Seyed-Mohsen Moosavi-Dezfooli, Alhussein Fawzi, Omar Fawzi, and Pascal Frossard. Universal adversarial perturbations. *CoRR*, abs/1610.08401, 2016.
- [57] A. Nagrani, J. S. Chung, and A. Zisserman. Voxceleb: a large-scale speaker identification dataset. In *INTERSPEECH*, 2017.
- [58] Muzammal Naseer, Salman H. Khan, Munawar Hayat, Fahad Shahbaz Khan, and Fatih Porikli. A self-supervised approach for adversarial robustness. In *2020 IEEE/CVF Conference on Computer Vision and Pattern Recognition, CVPR 2020*, pages 259–268. Computer Vision Foundation / IEEE, 2020.
- [59] Nicolas Papernot, Patrick D. McDaniel, Ian J. Goodfellow, Somesh Jha, Z. Berkay Celik, and Ananthram Swami. Practical black-box attacks against machine learning. In Ramesh Karri, Ozgur Sinanoglu, Ahmad-Reza Sadeghi, and Xun Yi, editors, *AsiaCCS 2017*.
- [60] Nicolas Papernot, Patrick D. McDaniel, Xi Wu, Somesh Jha, and Ananthram Swami. Distillation as a defense to adversarial perturbations against deep neural networks. In *IEEE Symposium on Security and Privacy, SP 2016*, pages 582–597. IEEE Computer Society, 2016.
- [61] Zeyu Qin, Yanbo Fan, Hongyuan Zha, and Baoyuan Wu. Random noise defense against query-based black-box attacks. pages 7650–7663, 2021.
- [62] Ali Rahmati, Seyed-Mohsen Moosavi-Dezfooli, Pascal Frossard, and Huaiyu Dai. Geoda: a geometric framework for black-box adversarial attacks. In *Proceedings of the IEEE/CVF conference on computer vision and pattern recognition*, pages 8446–8455, 2020.
- [63] Mirco Ravanelli, Titouan Parcollet, Peter Plantinga, Aku Rouhe, Samuele Cornell, Loren Lugosch, Cem Subakan, Nauman Dawalatabad, Abdelwahab Heba, Jianyuan Zhong, Ju-Chieh Chou, Sung-Lin Yeh, Szu-Wei Fu, Chien-Feng Liao, Elena Rastorgueva, François Grondin, William Aris, Hwidong Na, Yan Gao, Renato De Mori, and Yoshua Bengio. SpeechBrain: A general-purpose speech toolkit, 2021. arXiv:2106.04624.
- [64] Olaf Ronneberger, Philipp Fischer, and Thomas Brox. U-net: Convolutional networks for biomedical image segmentation. In *Medical Image Computing and Computer-Assisted Intervention—MICCAI 2015: 18th International Conference, Munich, Germany, October 5-9, 2015, Proceedings, Part III 18*, pages 234–241. Springer, 2015.
- [65] Kevin Roth, Yannic Kilcher, and Thomas Hofmann. The odds are odd: A statistical test for detecting adversarial examples. In Kamalika Chaudhuri and Ruslan Salakhutdinov, editors, *Proceedings of the 36th International Conference on Machine Learning, ICML 2019*, volume 97 of *Proceedings of Machine Learning Research*, pages 5498–5507. PMLR, 2019.
- [66] Olga Russakovsky, Jia Deng, Hao Su, Jonathan Krause, Sanjeev Satheesh, Sean Ma, Zhiheng Huang, Andrej Karpathy, Aditya Khosla, Michael Bernstein, Alexander C. Berg, and Li Fei-Fei. ImageNet Large Scale Visual Recognition Challenge. *International Journal of Computer Vision (IJCV)*, 115(3):211–252, 2015.

- [67] Pouya Samangouei, Maya Kabkab, and Rama Chellappa. Defense-gan: Protecting classifiers against adversarial attacks using generative models. In *6th International Conference on Learning Representations, ICLR 2018*, 2018.
- [68] Lukas Schott, Jonas Rauber, Matthias Bethge, and Wieland Brendel. Towards the first adversarially robust neural network model on MNIST. In *7th International Conference on Learning Representations, ICLR 2019, New Orleans, LA, USA, May 6–9, 2019*. OpenReview.net, 2019.
- [69] Ali Shafahi, Mahyar Najibi, Amin Ghiasi, Zheng Xu, John P. Dickerson, Christoph Studer, Larry S. Davis, Gavin Taylor, and Tom Goldstein. Adversarial training for free! In Hanna M. Wallach, Hugo Larochelle, Alina Beygelzimer, Florence d’Alché-Buc, Emily B. Fox, and Roman Garnett, editors, *Advances in Neural Information Processing Systems 32: Annual Conference on Neural Information Processing Systems 2019, NeurIPS 2019*, pages 3353–3364, 2019.
- [70] Yucheng Shi, Siyu Wang, and Yahong Han. Curls & whys: Boosting black-box adversarial attacks. In *IEEE Conference on Computer Vision and Pattern Recognition, CVPR 2019*, pages 6519–6527, 2019.
- [71] Karen Simonyan and Andrew Zisserman. Very deep convolutional networks for large-scale image recognition. In Yoshua Bengio and Yann LeCun, editors, *3rd International Conference on Learning Representations, ICLR 2015, San Diego, CA, USA, May 7–9, 2015, Conference Track Proceedings*, 2015.
- [72] Yang Song, Taesup Kim, Sebastian Nowozin, Stefano Ermon, and Nate Kushman. Pixeldefend: Leveraging generative models to understand and defend against adversarial examples. In *6th International Conference on Learning Representations, ICLR 2018*. OpenReview.net, 2018.
- [73] Jiaye Teng, Guang-He Lee, and Yang Yuan.  $\ell_1$  adversarial robustness certifies: a randomized smoothing approach. 2019.
- [74] Florian Tramèr. Detecting adversarial examples is (nearly) as hard as classifying them. In *ICML 2022*.
- [75] Florian Tramèr and Dan Boneh. Adversarial training and robustness for multi-perturbations. In Hanna M. Wallach, Hugo Larochelle, Alina Beygelzimer, Florence d’Alché-Buc, Emily B. Fox, and Roman Garnett, editors, *Advances in Neural Information Processing Systems, NeurIPS 2019*, pages 5858–5868, 2019.
- [76] Florian Tramèr, Alexey Kurakin, Nicolas Papernot, Ian J. Goodfellow, Dan Boneh, and Patrick D. McDaniel. Ensemble adversarial training: Attacks and defenses. In *ICLR 2018*.
- [77] Laurens Van der Maaten and Geoffrey Hinton. Visualizing data using t-sne. *Journal of machine learning research*, 9(11), 2008.
- [78] Viet Quoc Vo, Ehsan Abbasnejad, and Damith Ranasinghe. Query efficient decision based sparse attacks against black-box deep learning models. In *The Tenth International Conference on Learning Representations, ICLR 2022, Virtual Event, April 25–29, 2022*. OpenReview.net, 2022.
- [79] Eric Wong and J. Zico Kolter. Provable defenses against adversarial examples via the convex outer adversarial polytope. In Jennifer G. Dy and Andreas Krause, editors, *Proceedings of the 35th International Conference on Machine Learning, ICML 2018*, volume 80 of *Proceedings of Machine Learning Research*, pages 5283–5292. PMLR, 2018.
- [80] Eric Wong, Frank R. Schmidt, and J. Zico Kolter. Wasserstein adversarial examples via projected sinkhorn iterations. In Kamalika Chaudhuri and Ruslan Salakhutdinov, editors, *Proceedings of the 36th International Conference on Machine Learning, ICML 2019*, volume 97 of *Proceedings of Machine Learning Research*, pages 6808–6817. PMLR, 2019.
- [81] Cihang Xie, Jianyu Wang, Zhishuai Zhang, Zhou Ren, and Alan L. Yuille. Mitigating adversarial effects through randomization. In *6th International Conference on Learning Representations, ICLR 2018*. OpenReview.net, 2018.
- [82] Saining Xie, Ross B. Girshick, Piotr Dollár, Zhuowen Tu, and Kaiming He. Aggregated residual transformations for deep neural networks. In *2017 IEEE Conference on Computer Vision and Pattern Recognition, CVPR 2017, Honolulu, HI, USA, July 21–26, 2017*, pages 5987–5995. IEEE Computer Society, 2017.
- [83] Shangyu Xie, Han Wang, Yu Kong, and Yuan Hong. Universal 3-dimensional perturbations for black-box attacks on video recognition systems. In *In Proceedings of the 43rd IEEE Symposium on Security and Privacy, 2022*.
- [84] Weilin Xu, David Evans, and Yanjun Qi. Feature squeezing: Detecting adversarial examples in deep neural networks. *arXiv preprint arXiv:1704.01155*, 2017.
- [85] Greg Yang, Tony Duan, J. Edward Hu, Hadi Salman, Ilya P. Razenshteyn, and Jerry Li. Randomized smoothing of all shapes and sizes. In *ICML*, volume 119 of *Proceedings of Machine Learning Research*, pages 10693–10705. PMLR, 2020.
- [86] Sergey Zagoruyko and Nikos Komodakis. Wide residual networks. In Richard C. Wilson, Edwin R. Hancock, and William A. P. Smith, editors, *Proceedings of the British Machine Vision Conference 2016, BMVC 2016, York, UK, September 19–22, 2016*. BMVA Press, 2016.
- [87] Hongyang Zhang, Yaodong Yu, Jiantao Jiao, Eric Xing, Laurent El Ghaoui, and Michael Jordan. Theoretically principled trade-off between robustness and accuracy. In *International conference on machine learning*, pages 7472–7482. PMLR, 2019.
- [88] Jiawei Zhang, Zhongzhu Chen, Huan Zhang, Chaowei Xiao, and Bo Li. {DiffSmooth}: Certifiably robust learning via diffusion models and local smoothing. In *32nd USENIX Security Symposium (USENIX Security 23)*, pages 4787–4804, 2023.

## A PROOFS

### A.1 Proof of Theorem 1

The proof of Theorem 1 is based on the Neyman-Pearson Lemma, so we first review the Neyman-Pearson Lemma.

LEMMA 1. (**Neyman-Pearson Lemma**) *Let  $X$  and  $Y$  be random variables in  $\mathbb{R}^d$  with densities  $\mu_X$  and  $\mu_Y$ . Let  $f : \mathbb{R}^d \rightarrow \{0, 1\}$  be a random or deterministic function. Then:*

(1) *If  $S = \{z \in \mathbb{R}^d : \frac{\mu_Y(z)}{\mu_X(z)} \leq t\}$  for some  $t > 0$  and  $\mathbb{P}(f(X) = 1) \geq \mathbb{P}(X \in S)$ , then  $\mathbb{P}(f(Y) = 1) \geq \mathbb{P}(Y \in S)$ ;*

(2) *If  $S = \{z \in \mathbb{R}^d : \frac{\mu_Y(z)}{\mu_X(z)} \geq t\}$  for some  $t > 0$  and  $\mathbb{P}(f(X) = 1) \leq \mathbb{P}(X \in S)$ , then  $\mathbb{P}(f(Y) = 1) \leq \mathbb{P}(Y \in S)$ .*

Let  $x \in \mathbb{R}^d$  be any clean input with label  $y$ . Let noise  $\epsilon$  be drawn from any continuous distribution  $\varphi(0, \kappa)$ . Let  $x' \in \mathbb{R}^d$  be any input. Denote  $X = x' + \epsilon$ , and  $X_\delta = x' + \delta + \epsilon$ . Let  $f : \mathbb{R}^d \rightarrow \mathbb{R}^1$  be any deterministic or random function. For each input  $x$ , we can consider two classes:  $y$  or  $\neq y$ , so the problem can be considered as a binary classification problem. Let the lower bound of randomized parallel query on  $x'$  denoted as  $Q(x') = p_{adv}$ . Define the half set:

$$A := \{z : \frac{\varphi(z - \delta, \kappa)}{\varphi(z, \kappa)} \leq \tau\} \quad (9)$$

where the auxiliary parameter  $\tau$  is picked to suffice:

$$\mathbb{P}(X \in A) = \mathbb{P}\left[\frac{\varphi(x' + \epsilon - \delta, \kappa)}{\varphi(x' + \epsilon, \kappa)} \leq \tau\right] = p_{adv} \quad (10)$$

Suppose  $p_{adv}$  and the ASP Threshold  $p$  satisfy  $p_{adv} \geq p$ , then

$$\mathbb{P}[f(X) \neq y] \geq p_{adv} = \mathbb{P}(X \in A) \quad (11)$$

Using Neyman-Pearson Lemma (considering  $X_\delta = X + \delta$  as  $Y$  in Neyman-Pearson Lemma, and  $\neq y$  as class 1), we have:

$$\mathbb{P}[f(X_\delta) \neq y] \geq \mathbb{P}[X_\delta \in A] \quad (12)$$

which is equal to

$$\mathbb{P}[f(X_\delta) \neq y] \geq \mathbb{P}\left[\frac{\varphi(x' + \epsilon, \kappa)}{\varphi(x' + \epsilon + \delta, \kappa)} \leq \tau\right] \quad (13)$$

If  $\mathbb{P}\left(\frac{\varphi(x' + \epsilon, \kappa)}{\varphi(x' + \epsilon + \delta, \kappa)} \leq \tau\right) \geq p$ , we can guarantee that

$$\mathbb{P}[f(X_\delta) \neq y] \geq p \quad (14)$$

which means the probability of classifying  $X_\delta$  as adversarial examples is greater than  $p$ . Therefore, the distribution of  $X_\delta$  can be guaranteed to have the attack success probability larger than  $p$ .

Considering Eq. (10), we have  $\tau = \Phi^{-1}(p_{adv})$ , where  $\Phi^{-1}$  is the inverse CDF of random variable  $\frac{\varphi(x' + \epsilon - \delta, \kappa)}{\varphi(x' + \epsilon, \kappa)}$ . Therefore, substitute  $\tau$  in  $\mathbb{P}\left[\frac{\varphi(x' + \epsilon, \kappa)}{\varphi(x' + \epsilon + \delta, \kappa)} \leq \tau\right] \geq p$ , we have

$$\Phi_+[\Phi^{-1}(p_{adv})] \geq p \quad (15)$$

where  $\Phi_+$  is the CDF of random variable  $\frac{\varphi(x' + \epsilon, \kappa)}{\varphi(x' + \epsilon + \delta, \kappa)}$ . The ratios can be further simplified as

$$\frac{\varphi(x' + \epsilon - \delta, \kappa)}{\varphi(x' + \epsilon, \kappa)} = \frac{\varphi(\epsilon - \delta, \kappa)}{\varphi(\epsilon, \kappa)} \quad (16)$$

$$\frac{\varphi(x' + \epsilon, \kappa)}{\varphi(x' + \epsilon + \delta, \kappa)} = \frac{\varphi(\epsilon, \kappa)}{\varphi(\epsilon + \delta, \kappa)} \quad (17)$$

Now we complete the proof of Theorem 1.

## A.2 Certifiable Attack: Gaussian Noise

COROLLARY 2.1. (*Certifiable Adversarial Shifting: Gaussian Noise*) Under the same condition with Theorem 1, and let  $\epsilon$  be a noise drawn from Gaussian distribution  $\mathcal{N}(0, \sigma)$ . Then, if the randomized query on the adversarial input satisfies Eq. (5):

$$\mathbb{P}[f(x' + \epsilon) \neq y] \geq \underline{p}_{adv} = Q(x') \geq p \quad (18)$$

Then  $\mathbb{P}[f(x' + \delta + \epsilon) \neq y] \geq p$  is guaranteed for any shifting vector  $\delta$  when

$$\|\delta\|_2 \leq \sigma[\Phi^{-1}(\underline{p}_{adv}) - \Phi^{-1}(p)] \quad (19)$$

where  $\Phi^{-1}$  denotes the inverse of the standard Gaussian CDF.

PROOF. The Gaussian distribution is  $\mu(x) \propto e^{-\frac{x^2}{2\sigma^2}}$ , thus

$$\frac{\mu(x - \delta)}{\mu(x)} = e^{(2x\delta - \delta^2)/(2\sigma^2)} \quad (20)$$

Let  $\tau := \exp((2\Phi_{\sigma}^{-1}(\underline{p}_{adv})\delta - \delta^2)/(2\sigma^2))$ , where  $\Phi_{\sigma}^{-1}$  denotes the inverse Gaussian CDF with variance  $\sigma$ . Let random variables  $X := x' + \epsilon$  and  $X_{\delta} := x' + \epsilon + \delta$ . Then we have:

$$\mathbb{P}(X \in A) = \mathbb{P}\left[\frac{\mu(X - \delta)}{\mu(X)} \leq \tau\right] \quad (21)$$

$$= \mathbb{P}[\exp((2X\delta - \delta^2)/(2\sigma^2))] \leq \quad (22)$$

$$\exp[(2\Phi_{\sigma}^{-1}(\underline{p}_{adv})\delta - \delta^2)/(2\sigma^2)] \quad (23)$$

$$= \mathbb{P}[X \leq \Phi_{\sigma}^{-1}(\underline{p}_{adv})] \quad (24)$$

$$= \underline{p}_{adv} \quad (25)$$

$$(26)$$

Using Neyman-Pearson Lemma, we have:

$$\mathbb{P}[f(X_{\delta}) \neq y] \geq \mathbb{P}[(X_{\delta}) \in A] \quad (27)$$

Since

$$\mathbb{P}[X_{\delta} \in A] = \mathbb{P}\left[\frac{\mu(X)}{\mu(X + \delta)} \leq \tau\right] \quad (28)$$

$$= \mathbb{P}[\exp((2X\delta + \delta^2)/(2\sigma^2))] \leq \quad (29)$$

$$\exp[(2\Phi_{\sigma}^{-1}(\underline{p}_{adv})\delta - \delta^2)/(2\sigma^2)] \quad (30)$$

$$= \mathbb{P}[2X\delta + \delta^2 \leq (2\Phi_{\sigma}^{-1}(\underline{p}_{adv})\delta - \delta^2)] \quad (31)$$

$$= \mathbb{P}[X \leq \Phi_{\sigma}^{-1}(\underline{p}_{adv}) - \|\delta\|] \quad (32)$$

$$= \mathbb{P}\left[\frac{X}{\sigma} \leq \Phi^{-1}(\underline{p}_{adv}) - \frac{\|\delta\|}{\sigma}\right] \quad (33)$$

where  $\Phi^{-1}$  denotes the inverse standard Gaussian CDF.

To guarantee that  $\mathbb{P}[f(X_{\delta}) \neq y] \geq p$ , we need:

$$\mathbb{P}[X_{\delta} \in A] = \mathbb{P}\left[\frac{X}{\sigma} \leq \Phi^{-1}(\underline{p}_{adv}) - \frac{\|\delta\|}{\sigma}\right] \quad (34)$$

$$\geq p \quad (35)$$

$$(36)$$

which is equivalent to

$$\|\delta\| \leq \sigma[\Phi^{-1}(\underline{p}_{adv}) - \Phi^{-1}(p)] \quad (37)$$

This completes the proof of Corollary 2.1.  $\square$

## A.3 Proof of Theorem 2

If the Condition Eq. (5) is satisfied, we have

$$\underline{p}_{adv} \geq p \quad (38)$$

For any direction  $w$ , our goal is to find the  $\delta$  in this direction with maximum  $\|\delta\|_2$ . When  $\|\delta\|_2 = 0$ , we have

$$\Phi_+ = \Phi_- \quad (39)$$

Thus, we have

$$\Phi_+[\Phi_{-}^{-1}(\underline{p}_{adv})] = \underline{p}_{adv} \geq p \quad (40)$$

Then, we prove that when  $\|\delta\|_2$  increase, we will get  $\Phi_+[\Phi_{-}^{-1}(\underline{p}_{adv})]$  decrease.

Since  $\Phi_-$  is the CDF of the random variable  $\frac{\varphi(\epsilon - \delta, \kappa)}{\varphi(\epsilon, \kappa)}$ , and  $\varphi(x)$  decreases when  $|x|$  increases, when  $\|\delta\|_2 \rightarrow \infty$ , we have  $\frac{\varphi(\epsilon - \delta, \kappa)}{\varphi(\epsilon, \kappa)} \rightarrow 0$ , and  $\Phi_{-}^{-1}(\underline{p}_{adv}) \rightarrow 0$ .

Since  $\Phi_+$  is the CDF of the random variable  $\frac{\varphi(\epsilon, \kappa)}{\varphi(\epsilon + \delta, \kappa)}$ , when  $\|\delta\|_2 \rightarrow \infty$ ,  $\frac{\varphi(\epsilon, \kappa)}{\varphi(\epsilon + \delta, \kappa)} \rightarrow \infty$ , so  $\Phi_+ \rightarrow 0$ .

Therefore, when  $\|\delta\|_2 \rightarrow \infty$ , we have

$$\Phi_+[\Phi_{-}^{-1}(\underline{p}_{adv})] \rightarrow 0 < p \quad (41)$$

When  $\|\delta\|_2 \rightarrow 0$ , we have

$$\Phi_+[\Phi_{-}^{-1}(\underline{p}_{adv})] = \underline{p}_{adv} \geq p \quad (42)$$

Since  $\Phi_-$  and  $\Phi_+$  is continuous function, between 0 and  $\infty$ , there must be some  $\delta$  such that  $\Phi_+[\Phi_{-}^{-1}(\underline{p}_{adv})] = p$ .

Now we prove that the binary search algorithm can always find the  $\delta$  solution, then we show how to bound the adversarial attack certification. We use Monte Carlo method to estimate the  $\underline{p}_{adv}$  as well as the CDFs  $\Phi_-$  and  $\Phi_+$ . To bound the empirical CDFs, we leverage Dvoretzky-Kiefer-Wolfowitz inequality [27].

LEMMA 2. (*Dvoretzky-Kiefer-Wolfowitz inequality (restate)*) Let  $X_1, X_2, \dots, X_n$  be real-valued independent and identically distributed random variables with cumulative distribution function  $F(\cdot)$ , where  $n \in \mathbb{N}$ . Let  $F_n$  denote the associated empirical distribution function defined by

$$F_n(x) = \frac{1}{n} \sum_{i=1}^n \mathbf{1}_{\{X_i \leq x\}}, x \in \mathbb{R} \quad (43)$$

The Dvoretzky-Kiefer-Wolfowitz inequality bounds the probability that the random function  $F_n$  differs from  $F$  by more than a given constant  $\Delta \in \mathbb{R}^+$ :

$$\mathbb{P}\left[\sup_{x \in \mathbb{R}} |F_n(x) - F(x)| > \Delta\right] \leq 2e^{-2n\Delta^2} \quad (44)$$

Let the Monte Carlo sampling number  $N_m$ . Each shifting is an independent certification, and there are a lower-bound estimation and two CDF estimations in each certification. Suppose the confidence of lower-bound estimation is  $(1 - \alpha)$ , then the certification confidence should be at least  $(1 - \alpha)(1 - 2e^{-2N_m\Delta^2})^2$ .



## B DENOISING WITH DIFFUSION MODELS

The certifiable adversarial examples sampled from *Adversarial Distribution* are noise-injected inputs that still might be perceptible when the noise is large. We further leverage the recent innovation for image synthesis, i.e., diffusion model [35], to denoise the adversarial examples for better imperceptibility. The key idea is to consider the noise-perturbed adversarial examples as the middle sample in the forward process of the diffusion model [11, 88]. This is shown to improve the imperceptibility and the diversity of the adversarial examples.

Specifically, the closed-form sampling in the forward process at timestep  $t$  in [35] can be written as:

$$x_t = \sqrt{\bar{\alpha}_t}x_0 + \sqrt{1 - \bar{\alpha}_t}\epsilon_0 \quad (45)$$

where  $x_0 = x$  is a clean image,  $\bar{\alpha}_t$  is the parameter indicating the transformation of the image in the forward process, and  $\epsilon_0$  is a noise drawn from the standard normal distribution  $\mathcal{N}(0, 1)$ . The certifiable adversarial examples when adding noise  $\epsilon_0$  can be expressed as:

$$x_{adv} = x' + \delta + \epsilon_0 \quad (46)$$

We can then consider  $x_{adv}$  as the sample  $x_t$  in Eq. (45) by transforming  $x_{adv}$  to  $\sqrt{\bar{\alpha}_t}x_{adv}$  and satisfying these conditions: (1)  $x' + \delta = x_0$  and (2)  $\sqrt{\bar{\alpha}_t}\sigma = \sqrt{1 - \bar{\alpha}_t}$ . Then, we have  $\bar{\alpha}_t = \frac{1}{\sigma^2+1}$  to bridge diffusion model and the certifiable attack.

By finding the corresponding time step  $t$  and  $\bar{\alpha}_t$ , we can leverage the reverse process  $\mathcal{R}(\cdot)$  of the diffusion model to denoise  $x_{adv}$ :

$$x'_{adv} = \mathcal{R}(\mathcal{R}(\dots\mathcal{R}(\sqrt{\bar{\alpha}_t}x_{adv}))) \quad (47)$$

Note that the reverse denoising process can be plugged into our attack framework by simply replacing  $x_{adv}$  with  $x'_{adv}$  in all processes. It will not affect the guarantee since the denoising process can be part of the classification model, i.e., constructing a new target model  $f'(x_{adv}) = f(\mathcal{R}(\dots\mathcal{R}(\sqrt{\bar{\alpha}_t}x_{adv})))$  given any  $f$ .

## C ADVERSARIAL EXAMPLE VISUALIZATION

We visualize the adversarial examples  $x_{adv} \varphi(x', \kappa)$  during the crafting of Certifiable Attack for Binary-search Localization 6 and SSSP Localization 7. It shows that when  $\sigma = 0.025$ , both the Binary-search and SSSP-based certifiable attack can craft imperceptible perturbations. The difference is that the binary search method starts from a random  $x'$  and requires more # RPQ to update the *Adversarial Distribution*, while the SSSP can easily find an initial *Adversarial Distribution* with small perturbation and thus requires fewer # RPQ.

## D ADDITIONAL EXPERIMENTS

### D.1 Additional Experimental Settings

Table 12 summarizes all parameter settings.

### D.2 More Results Black-Box Attacks against the 4 SOTA Defenses

*D.2.1 More Results on Attacking Blacklight.* See Results in Table 13-Table 20.

*D.2.2 More Results on Attacking RAND-Pre.* See Results in Table 21-Table 28.

*D.2.3 More Results on Attacking RAND-Post.* See Results in Table 29-Table 36.

### D.3 Attacking Other Empirical and Certified Defenses

*D.3.1 Attacking Empirical Feature Squeezing Detection.* We also evaluate the certifiable attack against adversarial detection. Specifically, we select the Feature Squeezing [84] method, which modifies the image and detects the adversarial examples according to the difference of model outputs. To position the performance of the detection, we compare the certifiable attack with the C&W empirical attack [12]. In this experiment, Gaussian noise was adopted, and parameters are set as  $\sigma = 0.25$  and  $p = 90\%$ . We draw the ROC curve in Figure 8. As the results show, the certifiable attack is less detectable than the C&W attack w.r.t. Feature Squeezing (with lower ROC scores), possibly because the prediction of empirical adversarial examples is less robust to image modification (empirical adversarial examples tend to be some special data points near the decision boundary). After the modification, it tends to output a different result. The outputs of certifiable adversarial examples are more consistent after the modification since their neighbors tend to be adversarial as well.

*D.3.2 Attacking Randomized Smoothing-based Certified Defense.* Randomized smoothing trains the classifier on inputs with Gaussian noises. We evaluate the certifiable attack on the classifier trained with the same noise. Specifically, we use the Gaussian noise with  $\sigma = 0.12$  to 0.50 in the classifier training and  $\sigma = 0.25$  in the certifiable attack. Table 37 shows that the noise-trained classifier, especially when the model is trained with the same noise parameter as the adversary, can significantly degrade the performance of certifiable attacks. Noticeably, the smoothed training increases the perturbation sizes, especially the Mean Dist.  $\ell_2$  significantly, and doubles the number of RPQ, which means the smoothing training can obstacle the certifiable attack to find a *Adversarial Distribution*. It also reduces the certified accuracy of the certifiable attack significantly. However, the certifiable attack can still guarantee that 87.20% of the test samples can be provably misclassified. Without performing the randomized smoothing certification against the certifiable attack, we can conclude that the certified accuracy of randomized smoothing with  $\sigma = 0.25$  will be at most 12.80% since at least 87.20% of the RandAEs are guaranteed to generate successful AEs with 90% probability.

### D.4 Diffusion Model for Denoising

We implement the diffusion model [35] with the linear schedule. We train a diffusion model and an UNet with  $3 \times 32 \times 32$  dimension for CIFAR10 and  $3 \times 64 \times 64$  dimension for ImageNet and denoise the certified *Adversarial Distributions* samples injected by Gaussian noise with  $\sigma = 0.25$ . The experimental results are shown in Table 38. Although the diffusion denoise increases the number of queries and Mean Dist.  $\ell_2$ , the perturbation of AE samples is significantly reduced due to the denoise. It is worth noting that the AEs generated by the diffusion model are unique due to the stochastic reverse process. This difference enables the certifiable attack to generate diverse AEs while ensuring the ASP guarantee.

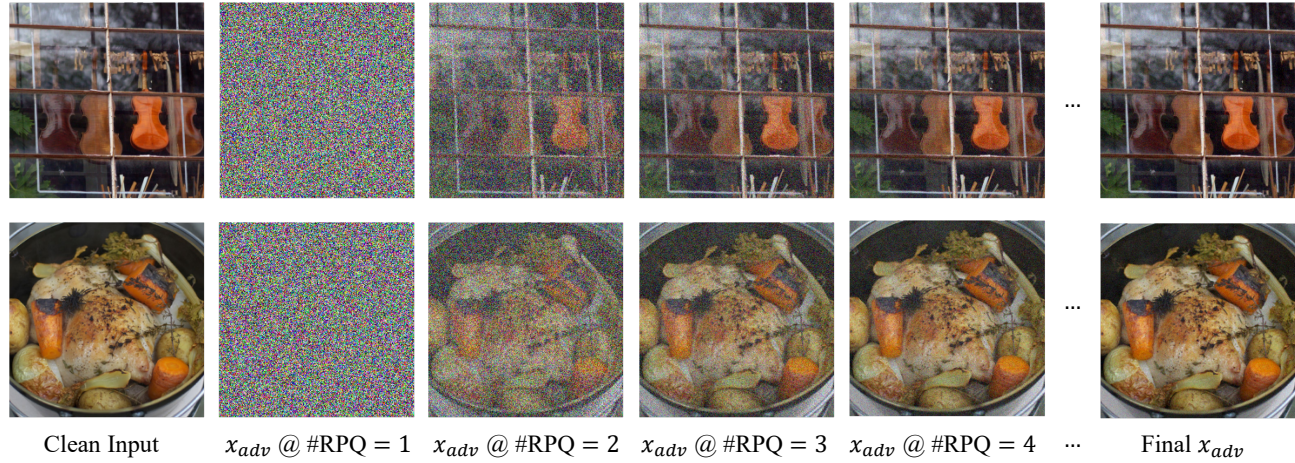


Figure 6: Visualization of Successful Adversarial Examples Crafting by Certifiable Attack with Binary-search Localization

Table 12: Summary of all parameter settings

Experiments	General		Random Parallel Query		Smoothed Self-supervised Localization					Bin-search Localization			Refinement					
	$p$	$\sigma$	$\alpha$	$N_m$	$\pi_{init}$	$\gamma$	$N_{max}$	$n_{max}$	$\eta$	$N_s$	$N_r$	$N_b$	$\Omega$	$M$	$\eta'$	$\epsilon$	$\epsilon_s$	$N_h$
Comparison with empirical attack under Blacklight detection	10%	0.025	0.001	50	3/255	3/255	85	10	3/255	50	85	15	0.1	20	0.05	0.01	0.0025	72
Comparison with empirical attack against RAND pre-processing defense	10%	0.025	0.001	50	3/255	3/255	85	10	3/255	50	85	15	0.1	20	0.05	0.01	0.0025	72
Comparison with empirical attack against RAND post-processing Defense	10%	0.025	0.001	50	3/255	3/255	85	10	3/255	50	85	15	0.1	20	0.05	0.01	0.0025	72
Comparison with empirical attack against TRADES adversarial training	10%	0.025	0.001	50	3/255	3/255	85	10	3/255	50	85	15	0.1	20	0.05	0.01	0.0025	72
Certifiable Attack against Feature Squeezing	90%	0.25	0.001	1000	3/255	3/255	85	10	3/255	1000	85	15	0.1	20	0.05	0.01	0.025	72
Certifiable Attack against Randomized Smoothing and Adaptive Denoiser	90%	0.25	0.001	1000	3/255	3/255	85	10	3/255	1000	85	15	0.1	20	0.05	0.01	0.025	72
Ablation study: Certifiable attack vs. different noise variance	90%	0.10 - 0.50	0.001	500/1000	3/255	3/255	85	10	3/255	500/1000	85	15	0.1	20	0.05	0.01	0.1 $\sigma$	72
Ablation study: Certifiable attack vs. different ASP Threshold $p$	50 - 95%	0.25	0.001	500/1000	3/255	3/255	85	10	3/255	500/1000	85	15	0.1	20	0.05	0.01	0.025	72
Ablation study: Certifiable attack vs. different Localization/Shifting	90%	0.25	0.001	500/1000	3/255	3/255	85	10	3/255	500/1000	85	15	0.1	20	0.05	0.01	0.025	72
Ablation study: Certifiable attack vs. different noise PDF	90%	-	0.001	500/1000	3/255	3/255	85	10	3/255	500/1000	85	15	0.1	20	0.05	0.01	-	72
Ablation study: Certifiable attack w/ and w/o Diffusion Denoise	90%	0.25	0.001	500/1000	3/255	3/255	85	10	3/255	500/1000	85	15	0.1	20	0.05	0.01	0.025	72

Table 13: Attack performance under Blacklight detection on VGG and CIFAR10 (Clean Accuracy: 90.3%)

Attack	Query Type	Pert. Type	Det. Rate %	# Q to Det.	Det. Cov. %	Model Acc.	# Q	Dist. $\ell_2$
Bandit	Score	$\ell_\infty$	100.0	1.0	69.2	0.0	59	4.77
NES	Score	$\ell_\infty$	100.0	8.6	21.2	0.0	264	1.33
Parsimonious	Score	$\ell_\infty$	100.0	2.0	96.7	0.0	107	4.90
Sign	Score	$\ell_\infty$	100.0	2.0	92.4	0.0	83	4.90
Square	Score	$\ell_\infty$	100.0	2.0	75.9	0.0	25	4.90
ZOSignSGD	Score	$\ell_\infty$	100.0	2.0	50.6	0.0	267	1.29
GeoDA	Label	$\ell_\infty$	100.0	1.0	89.7	0.2	377	3.08
HSJ	Label	$\ell_\infty$	100.0	7.7	92.2	0.0	353	2.94
Opt	Label	$\ell_\infty$	100.0	8.6	83.4	37.1	2571	1.04
RayS	Label	$\ell_\infty$	100.0	5.8	78.6	0.0	226	4.82
SignFlip	Label	$\ell_\infty$	100.0	8.7	56.0	0.0	68	3.91
SignOPT	Label	$\ell_\infty$	100.0	8.6	89.1	21.0	1112	1.15
Bandit	Score	$\ell_2$	100.0	1.0	98.9	0.0	121	2.62
NES	Score	$\ell_2$	100.0	8.5	32.6	0.0	823	0.53
Simple	Score	$\ell_2$	100.0	1.0	99.8	0.0	779	0.77
Square	Score	$\ell_2$	100.0	2.0	78.7	0.0	26	4.47
ZOSignSGD	Score	$\ell_2$	100.0	2.0	53.4	0.3	1631	0.48
Boundary	Label	$\ell_2$	100.0	7.6	67.4	21.7	315	2.70
GeoDA	Label	$\ell_2$	100.0	1.0	89.7	0.1	230	2.80
HSJ	Label	$\ell_2$	100.0	7.6	90.9	0.0	188	2.49
Opt	Label	$\ell_2$	100.0	8.6	65.1	32.6	675	2.39
SignOPT	Label	$\ell_2$	100.0	8.6	77.7	24.7	510	1.89
PointWise	Label	Opt.	100.0	1.0	99.5	0.0	764	2.06
SparseEvo	Label	Opt.	95.7	1.0	100.0	0.0	9569	2.40
CA (sssp)	Label	Opt.	0.0	$\infty$	0.0	6.2	393	3.75
CA (bin search)	Label	Opt.	0.0	$\infty$	0.0	0.0	473	5.20

Table 14: Attack performance under Blacklight detection on ResNet and CIFAR10 (Clean Accuracy: 92.1%)

Attack	Query Type	Pert. Type	Det. Rate %	# Q to Det.	Det. Cov. %	Model Acc.	# Q	Dist. $\ell_2$
Bandit	Score	$\ell_\infty$	100.0	1.0	67.9	0.0	32	4.90
NES	Score	$\ell_\infty$	100.0	8.5	20.7	0.0	256	1.36
Parsimonious	Score	$\ell_\infty$	100.0	2.0	96.3	0.0	83	5.01
Sign	Score	$\ell_\infty$	100.0	2.0	92.2	0.0	94	4.99
Square	Score	$\ell_\infty$	100.0	2.0	71.6	0.0	17	4.99
ZOSignSGD	Score	$\ell_\infty$	100.0	2.0	50.6	0.0	248	1.30
GeoDA	Label	$\ell_\infty$	100.0	1.0	89.6	9.8	215	2.84
HSJ	Label	$\ell_\infty$	100.0	361.1	85.2	0.5	683	3.17
Opt	Label	$\ell_\infty$	89.0	9.0	85.3	50.5	2290	0.86
RayS	Label	$\ell_\infty$	100.0	5.8	78.9	0.0	251	4.82
SignFlip	Label	$\ell_\infty$	99.5	246.8	56.3	0.5	389	4.22
SignOPT	Label	$\ell_\infty$	92.5	8.4	88.4	31.0	1270	1.08
Bandit	Score	$\ell_2$	100.0	1.0	98.7	0.0	109	2.65
NES	Score	$\ell_2$	100.0	8.1	32.5	0.0	762	0.53
Simple	Score	$\ell_2$	100.0	1.0	99.7	0.0	703	0.78
Square	Score	$\ell_2$	100.0	2.0	74.2	0.0	21	4.55
ZOSignSGD	Score	$\ell_2$	100.0	2.0	53.3	0.0	1340	0.45
Boundary	Label	$\ell_2$	100.0	341.4	71.5	35.4	438	2.38
GeoDA	Label	$\ell_2$	100.0	1.0	89.7	8.3	274	2.65
HSJ	Label	$\ell_2$	100.0	358.4	82.1	0.4	497	2.75
Opt	Label	$\ell_2$	90.1	9.9	64.4	40.0	660	2.34
SignOPT	Label	$\ell_2$	88.1	8.5	75.6	35.3	414	1.67
PointWise	Label	Opt.	91.3	1.0	99.6	8.0	888	1.92
SparseEvo	Label	Opt.	87.9	1.0	100.0	8.8	8796	2.57
CA (sssp)	Label	Opt.	0.0	$\infty$	0.0	8.3	437	3.95
CA (bin search)	Label	Opt.	0.0	$\infty$	0.0	10.7	421	4.09

**Table 15: Attack performance under Blacklight detection on ResNeXt and CIFAR10 (Clean Accuracy: 94.9%)**

Attack	Query Type	Pert. Type	Det. Rate %	# Q to Det.	Det. Cov. %	Model Acc.	# Q	Dist. $\ell_2$
Bandit	Score	$\ell_\infty$	100.0	1.0	67.3	0.0	27	5.07
NES	Score	$\ell_\infty$	100.0	8.5	20.4	0.0	213	1.28
Parsimonious	Score	$\ell_\infty$	100.0	2.0	97.3	0.0	104	5.16
Sign	Score	$\ell_\infty$	100.0	2.0	93.6	0.0	75	5.15
Square	Score	$\ell_\infty$	100.0	2.0	69.7	0.0	15	5.15
ZOSignSGD	Score	$\ell_\infty$	100.0	2.0	50.6	0.0	222	1.27
GeoDA	Label	$\ell_\infty$	100.0	1.0	89.9	10.1	197	2.22
HSJ	Label	$\ell_\infty$	100.0	148.1	85.9	0.0	383	2.65
Opt	Label	$\ell_\infty$	88.4	8.5	78.7	43.3	1644	0.87
RayS	Label	$\ell_\infty$	100.0	5.4	81.4	0.0	391	4.77
SignFlip	Label	$\ell_\infty$	100.0	165.8	41.5	0.0	205	3.43
SignOPT	Label	$\ell_\infty$	92.7	8.6	92.5	26.0	780	0.92
Bandit	Score	$\ell_2$	100.0	1.0	98.8	0.0	110	2.81
NES	Score	$\ell_2$	100.0	8.8	32.4	0.0	608	0.48
Simple	Score	$\ell_2$	100.0	1.0	99.7	0.0	595	0.71
Square	Score	$\ell_2$	100.0	2.0	74.2	0.0	20	4.69
ZOSignSGD	Score	$\ell_2$	100.0	2.0	53.4	0.6	1376	0.46
Boundary	Label	$\ell_2$	100.0	161.4	56.2	14.8	186	2.71
GeoDA	Label	$\ell_2$	100.0	1.0	90.3	10.2	165	2.13
HSJ	Label	$\ell_2$	100.0	138.3	83.9	0.0	287	2.16
Opt	Label	$\ell_2$	88.4	8.6	60.8	37.2	480	1.65
SignOPT	Label	$\ell_2$	88.4	8.6	87.5	32.7	387	1.17
PointWise	Label	Opt.	97.6	1.0	97.6	2.3	1084	2.01
SparseEvo	Label	Opt.	95.0	1.0	100.0	2.6	9506	3.11
CA (sssp)	Label	Opt.	0.0	$\infty$	0.0	8.3	437	3.95
CA (bin search)	Label	Opt.	0.0	$\infty$	0.0	10.7	421	4.09

**Table 17: Attack performance under Blacklight detection on VGG and CIFAR100 (Clean Accuracy: 68.6%)**

Attack	Query Type	Pert. Type	Det. Rate %	# Q to Det.	Det. Cov. %	Model Acc.	# Q	Dist. $\ell_2$
Bandit	Score	$\ell_\infty$	100.0	1.0	61.5	0.0	22	3.66
NES	Score	$\ell_\infty$	100.0	8.6	21.6	0.0	178	0.80
Parsimonious	Score	$\ell_\infty$	100.0	2.0	94.0	0.0	73	3.70
Sign	Score	$\ell_\infty$	100.0	2.0	84.6	0.0	44	3.68
Square	Score	$\ell_\infty$	100.0	2.0	64.7	0.0	9	3.68
ZOSignSGD	Score	$\ell_\infty$	100.0	2.0	50.7	0.1	184	0.79
GeoDA	Label	$\ell_\infty$	100.0	1.0	89.8	0.0	154	2.07
HSJ	Label	$\ell_\infty$	100.0	7.2	91.9	0.0	232	2.16
Opt	Label	$\ell_\infty$	100.0	8.6	74.7	20.8	1463	0.97
RayS	Label	$\ell_\infty$	100.0	6.6	71.7	0.0	120	4.40
SignFlip	Label	$\ell_\infty$	100.0	8.7	44.9	0.0	30	2.88
SignOPT	Label	$\ell_\infty$	100.0	8.5	92.3	23.0	699	0.84
Bandit	Score	$\ell_2$	100.0	1.0	97.9	0.0	73	1.35
NES	Score	$\ell_2$	100.0	8.7	32.4	0.0	553	0.31
Simple	Score	$\ell_2$	100.0	1.0	99.4	0.0	507	0.44
Square	Score	$\ell_2$	100.0	2.0	64.0	0.0	6	3.35
ZOSignSGD	Score	$\ell_2$	100.0	2.0	53.6	0.4	1137	0.29
Boundary	Label	$\ell_2$	100.0	7.3	54.0	6.3	100	2.49
GeoDA	Label	$\ell_2$	100.0	1.0	90.2	0.0	125	1.95
HSJ	Label	$\ell_2$	100.0	7.3	91.4	0.0	147	1.74
Opt	Label	$\ell_2$	100.0	8.6	63.3	19.8	563	1.51
SignOPT	Label	$\ell_2$	99.4	8.5	88.7	14.4	446	1.13
PointWise	Label	Opt.	100.0	1.0	98.9	0.0	300	1.42
SparseEvo	Label	Opt.	86.5	1.0	100.0	0.0	8647	1.88
CA (sssp)	Label	Opt.	0.0	$\infty$	0.0	1.7	187	2.34
CA (bin search)	Label	Opt.	0.0	$\infty$	0.0	0.0	457	2.70

**Table 16: Attack performance under Blacklight detection on WRN and CIFAR10 (Clean Accuracy: 96.1%)**

Attack	Query Type	Pert. Type	Det. Rate %	# Q to Det.	Det. Cov. %	Model Acc.	# Q	Dist. $\ell_2$
Bandit	Score	$\ell_\infty$	100.0	1.0	67.4	0.0	47	5.09
NES	Score	$\ell_\infty$	100.0	8.7	20.7	0.0	295	1.44
Parsimonious	Score	$\ell_\infty$	100.0	2.0	97.6	0.2	140	5.22
Sign	Score	$\ell_\infty$	100.0	2.0	94.6	0.0	130	5.21
Square	Score	$\ell_\infty$	100.0	2.0	74.5	0.0	21	5.21
ZOSignSGD	Score	$\ell_\infty$	100.0	2.0	50.6	0.2	300	1.42
GeoDA	Label	$\ell_\infty$	100.0	1.0	89.6	0.1	323	2.83
HSJ	Label	$\ell_\infty$	100.0	7.3	91.9	0.0	280	2.69
Opt	Label	$\ell_\infty$	97.0	11.3	81.1	35.0	2179	1.15
RayS	Label	$\ell_\infty$	100.0	4.9	81.5	0.0	309	4.87
SignFlip	Label	$\ell_\infty$	100.0	8.3	53.0	0.0	72	3.75
SignOPT	Label	$\ell_\infty$	88.4	8.5	89.4	28.0	843	0.97
Bandit	Score	$\ell_2$	100.0	1.0	98.8	0.0	136	2.71
NES	Score	$\ell_2$	100.0	8.2	32.5	0.0	863	0.57
Simple	Score	$\ell_2$	100.0	1.0	99.8	0.0	813	0.83
Square	Score	$\ell_2$	100.0	2.0	73.2	0.0	20	4.75
ZOSignSGD	Score	$\ell_2$	100.0	2.0	53.3	2.3	1803	0.54
Boundary	Label	$\ell_2$	100.0	7.3	62.2	16.7	376	2.85
GeoDA	Label	$\ell_2$	100.0	1.0	89.6	0.0	186	2.63
HSJ	Label	$\ell_2$	100.0	7.4	91.0	0.0	185	2.27
Opt	Label	$\ell_2$	97.3	10.7	66.3	35.1	678	2.14
SignOPT	Label	$\ell_2$	91.7	8.5	80.3	33.0	470	1.57
PointWise	Label	Opt.	99.9	1.0	99.5	0.1	800	1.96
SparseEvo	Label	Opt.	97.7	1.0	100.0	0.2	9772	2.83
CA (sssp)	Label	Opt.	0.0	$\infty$	0.0	6.8	417	3.7
CA (bin search)	Label	Opt.	0.0	$\infty$	0.0	0.0	461	5.05

**Table 18: Attack performance under Blacklight detection on ResNet and CIFAR100 (Clean Accuracy: 66.8%)**

Attack	Query Type	Pert. Type	Det. Rate %	# Q to Det.	Det. Cov. %	Model Acc.	# Q	Dist. $\ell_2$
Bandit	Score	$\ell_\infty$	100.0	1.0	62.5	0.0	10	3.56
NES	Score	$\ell_\infty$	100.0	8.5	21.3	0.0	141	0.72
Parsimonious	Score	$\ell_\infty$	100.0	2.0	93.5	0.0	49	3.61
Sign	Score	$\ell_\infty$	100.0	2.0	82.4	0.0	31	3.59
Square	Score	$\ell_\infty$	100.0	2.0	66.2	0.0	8	3.58
ZOSignSGD	Score	$\ell_\infty$	100.0	2.0	50.7	0.0	148	0.70
GeoDA	Label	$\ell_\infty$	100.0	1.0	89.5	0.0	152	2.21
HSJ	Label	$\ell_\infty$	100.0	7.3	91.8	0.0	214	2.23
Opt	Label	$\ell_\infty$	100.0	8.5	75.1	25.8	1442	0.96
RayS	Label	$\ell_\infty$	100.0	6.6	70.3	0.0	109	4.02
SignFlip	Label	$\ell_\infty$	100.0	8.7	49.0	0.0	39	3.28
SignOPT	Label	$\ell_\infty$	100.0	8.5	89.5	17.0	749	0.88
Bandit	Score	$\ell_2$	100.0	1.0	97.8	0.0	63	1.25
NES	Score	$\ell_2$	100.0	8.7	32.5	0.0	404	0.27
Simple	Score	$\ell_2$	100.0	1.0	99.5	0.0	371	0.39
Square	Score	$\ell_2$	100.0	2.0	64.4	0.0	6	3.26
ZOSignSGD	Score	$\ell_2$	100.0	2.0	53.5	0.1	747	0.23
Boundary	Label	$\ell_2$	100.0	7.3	56.4	9.1	105	2.67
GeoDA	Label	$\ell_2$	100.0	1.0	89.9	0.0	130	2.02
HSJ	Label	$\ell_2$	100.0	7.3	91.2	0.0	151	1.81
Opt	Label	$\ell_2$	100.0	8.5	63.2	21.6	567	1.58
SignOPT	Label	$\ell_2$	100.0	8.5	85.8	17.3	472	1.20
PointWise	Label	Opt.	100.0	1.0	99.2	0.0	468	1.52
SparseEvo	Label	Opt.	90.9	1.0	100.0	0.0	9088	2.18
CA (sssp)	Label	Opt.	0.0	$\infty$	0.0	1.4	191	2.39
CA (bin search)	Label	Opt.	0.0	$\infty$	0.0	0.0	458	3.05

**Table 19: Attack performance under Blacklight detection on ResNeXt and CIFAR100 (Clean Accuracy: 80.0%)**

Attack	Query Type	Pert. Type	Det. Rate %	# Q to Det.	Det. Cov. %	Model Acc.	# Q	Dist. $\ell_2$
Bandit	Score	$\ell_\infty$	100.0	1.0	62.3	0.0	13	4.28
NES	Score	$\ell_\infty$	100.0	8.6	21.6	0.0	145	0.87
Parsimonious	Score	$\ell_\infty$	100.0	2.0	95.5	0.0	73	4.32
Sign	Score	$\ell_\infty$	100.0	2.0	87.7	0.0	47	4.30
Square	Score	$\ell_\infty$	100.0	2.0	63.7	0.0	7	4.30
ZOSignSGD	Score	$\ell_\infty$	100.0	2.0	50.7	0.0	158	0.89
GeoDA	Label	$\ell_\infty$	100.0	1.0	90.1	0.1	136	1.91
HSJ	Label	$\ell_\infty$	100.0	7.3	92.0	0.0	226	1.96
Opt	Label	$\ell_\infty$	99.0	8.6	73.5	32.1	1158	0.84
RayS	Label	$\ell_\infty$	100.0	6.5	75.2	0.0	175	4.44
SignFlip	Label	$\ell_\infty$	100.0	8.8	42.2	0.0	27	2.52
SignOPT	Label	$\ell_\infty$	98.8	8.5	92.7	14.0	616	0.79
Bandit	Score	$\ell_2$	100.0	1.0	98.0	0.0	69	1.62
NES	Score	$\ell_2$	100.0	8.7	31.7	0.0	420	0.33
Simple	Score	$\ell_2$	100.0	1.0	99.5	0.0	409	0.48
Square	Score	$\ell_2$	100.0	2.0	65.8	0.0	8	3.92
ZOSignSGD	Score	$\ell_2$	100.0	2.0	53.5	0.0	1029	0.33
Boundary	Label	$\ell_2$	100.0	7.3	51.1	5.7	53	2.26
GeoDA	Label	$\ell_2$	100.0	1.0	90.6	0.1	120	1.84
HSJ	Label	$\ell_2$	100.0	7.3	91.7	0.0	146	1.53
Opt	Label	$\ell_2$	99.0	8.6	62.1	21.7	537	1.46
SignOPT	Label	$\ell_2$	98.9	8.6	89.5	16.5	432	1.07
PointWise	Label	Opt.	100.0	1.0	99.4	0.0	766	1.80
SparseEvo	Label	Opt.	93.8	1.0	100	0.0	9376	2.53
CA (sssp)	Label	Opt.	0.0	$\infty$	0.0	2.1	174	2.31
CA (bin search)	Label	Opt.	0.0	$\infty$	0.0	0.0	459	2.61

**Table 20: Attack performance under Blacklight detection on WRN and CIFAR100 (Clean Accuracy: 79.4%)**

Attack	Query Type	Pert. Type	Det. Rate %	# Q to Det.	Det. Cov. %	Model Acc.	# Q	Dist. $\ell_2$
Bandit	Score	$\ell_\infty$	100.0	1.0	62.1	0.0	13	4.25
NES	Score	$\ell_\infty$	100.0	8.8	21.7	0.0	151	0.87
Parsimonious	Score	$\ell_\infty$	100.0	2.0	95.2	0.0	75	4.29
Sign	Score	$\ell_\infty$	100.0	2.0	87.2	0.0	54	4.26
Square	Score	$\ell_\infty$	100.0	2.0	65.1	0.0	10	4.26
ZOSignSGD	Score	$\ell_\infty$	100.0	2.0	50.6	0.0	159	0.87
GeoDA	Label	$\ell_\infty$	100.0	1.0	90.0	0.0	139	1.93
HSJ	Label	$\ell_\infty$	100.0	7.3	91.9	0.0	185	1.89
Opt	Label	$\ell_\infty$	100.0	8.6	73.8	24.1	1269	0.93
RayS	Label	$\ell_\infty$	100.0	6.0	74.1	0.0	165	4.20
SignFlip	Label	$\ell_\infty$	100.0	8.7	43.1	0.0	29	2.70
SignOPT	Label	$\ell_\infty$	100.0	8.6	92.9	19.0	624	0.75
Bandit	Score	$\ell_2$	100.0	1.0	97.7	0.0	70	1.54
NES	Score	$\ell_2$	100.0	8.9	31.8	0.0	442	0.32
Simple	Score	$\ell_2$	100.0	1.0	99.4	0.0	437	0.48
Square	Score	$\ell_2$	100.0	2.0	65.2	0.0	7	3.88
ZOSignSGD	Score	$\ell_2$	100.0	2.0	53.6	0.5	964	0.31
Boundary	Label	$\ell_2$	100.0	7.2	52.0	4.8	81	2.46
GeoDA	Label	$\ell_2$	100.0	1.0	90.4	0.0	120	1.86
HSJ	Label	$\ell_2$	100.0	7.3	91.5	0.0	143	1.55
Opt	Label	$\ell_2$	100.0	8.6	65.2	22.2	586	1.35
SignOPT	Label	$\ell_2$	99.9	8.5	89.0	16.7	456	1.04
PointWise	Label	Opt.	100.0	1.0	99.1	0.0	469	1.57
SparseEvo	Label	Opt.	91.4	1.0	100.0	0.0	9145	2.16
CA (sssp)	Label	Opt.	0.0	$\infty$	0.0	1.6	218	2.56
CA (bin search)	Label	Opt.	0.0	$\infty$	0.0	0.0	458	2.65

**Table 21: Attack performance under RAND Pre-processing Defense on VGG and CIFAR10 (Clean Accuracy: 87.7%)**

Attack	Query Type	Perturbation Type	# Query	Model Acc.	Dist. $\ell_2$
Bandit	Score	$\ell_\infty$	116	36.1	4.68
NES	Score	$\ell_\infty$	612	50.7	1.69
Parsimonious	Score	$\ell_\infty$	565	63.7	4.79
Sign	Score	$\ell_\infty$	257	55.3	4.75
Square	Score	$\ell_\infty$	91	32.9	4.80
ZOSignSGD	Score	$\ell_\infty$	644	49.9	1.72
GeoDA	Label	$\ell_\infty$	324	58.1	2.58
HSJ	Label	$\ell_\infty$	591	59.7	2.26
Opt	Label	$\ell_\infty$	957	87.3	0.25
RayS	Label	$\ell_\infty$	251	60.1	4.60
SignFlip	Label	$\ell_\infty$	365	51.1	3.31
SignOPT	Label	$\ell_\infty$	1411	82.0	0.30
Bandit	Score	$\ell_2$	773	76.5	3.36
NES	Score	$\ell_2$	1875	72.2	0.75
Simple	Score	$\ell_2$	1693	89.3	0.14
Square	Score	$\ell_2$	100	33.9	4.33
ZOSignSGD	Score	$\ell_2$	2840	78.3	0.63
Boundary	Label	$\ell_2$	43	54.4	2.46
GeoDA	Label	$\ell_2$	299	62.0	2.35
HSJ	Label	$\ell_2$	735	56.5	3.20
Opt	Label	$\ell_2$	807	69.4	1.92
SignOPT	Label	$\ell_2$	586	50.9	2.76
PointWise	Label	Optimized	2813	83.0	2.02
SparseEvo	Label	Optimized	9492	80.8	1.62
CA (sssp)	Label	Optimized	359	5.7	3.53
CA (bin search)	Label	Optimized	473	0.0	4.94

**Table 22: Attack performance under RAND Pre-processing Defense on ResNet and CIFAR10 (Clean Accuracy 92.3%)**

Attack	Query Type	Perturbation Type	# Query	Model Acc.	Dist. $\ell_2$
Bandit	Score	$\ell_\infty$	52	27.2	4.88
NES	Score	$\ell_\infty$	605	49.9	1.84
Parsimonious	Score	$\ell_\infty$	254	50.1	4.97
Sign	Score	$\ell_\infty$	394	58.3	4.85
Square	Score	$\ell_\infty$	32	21.4	4.95
ZOSignSGD	Score	$\ell_\infty$	674	51.4	1.86
GeoDA	Label	$\ell_\infty$	265	62.8	2.53
HSJ	Label	$\ell_\infty$	641	64.6	2.12
Opt	Label	$\ell_\infty$	655	88.2	0.18
RayS	Label	$\ell_\infty$	306	62.9	4.75
SignFlip	Label	$\ell_\infty$	902	56.5	3.33
SignOPT	Label	$\ell_\infty$	1086	85.6	0.24
Bandit	Score	$\ell_2$	747	76.0	3.45
NES	Score	$\ell_2$	1808	71.2	0.77
Simple	Score	$\ell_2$	2139	90.4	0.15
Square	Score	$\ell_2$	44	24.2	4.49
ZOSignSGD	Score	$\ell_2$	2822	77.6	0.64
Boundary	Label	$\ell_2$	46	60.1	2.25
GeoDA	Label	$\ell_2$	333	66.7	2.14
HSJ	Label	$\ell_2$	1163	56.7	3.45
Opt	Label	$\ell_2$	724	72.8	1.93
SignOPT	Label	$\ell_2$	442	59.1	2.47
PointWise	Label	Optimized	3804	86.5	2.02
SparseEvo	Label	Optimized	8709	87.3	1.78
CA (sssp)	Label	Optimized	406	8.1	3.80
CA (bin search)	Label	Optimized	417	10.8	3.89

**Table 23: Attack performance under RAND Pre-processing Defense on ResNeXt and CIFAR10 (Clean Accuracy: 89.6%)**

Attack	Query Type	Perturbation Type	# Query	Model Acc.	Dist. $\ell_2$
Bandit	Score	$\ell_\infty$	54	25.9	4.81
NES	Score	$\ell_\infty$	446	48.2	1.61
Parsimonious	Score	$\ell_\infty$	537	68.1	4.88
Sign	Score	$\ell_\infty$	454	63.8	4.75
Square	Score	$\ell_\infty$	90	24.2	4.91
ZOSignSGD	Score	$\ell_\infty$	487	49.4	1.64
GeoDA	Label	$\ell_\infty$	197	58.9	2.43
HSJ	Label	$\ell_\infty$	363	59.3	2.30
Opt	Label	$\ell_\infty$	771	89.8	0.30
RayS	Label	$\ell_\infty$	305	65.3	4.60
SignFlip	Label	$\ell_\infty$	334	54.0	2.91
SignOPT	Label	$\ell_\infty$	895	84.9	0.33
Bandit	Score	$\ell_2$	407	75.1	3.03
NES	Score	$\ell_2$	1611	74.6	0.70
Simple	Score	$\ell_2$	1692	90.2	0.14
Square	Score	$\ell_2$	123	34.0	4.41
ZOSignSGD	Score	$\ell_2$	2582	80.9	0.59
Boundary	Label	$\ell_2$	18	52.9	2.50
GeoDA	Label	$\ell_2$	146	58.9	2.32
HSJ	Label	$\ell_2$	593	57.7	2.86
Opt	Label	$\ell_2$	694	76.1	1.58
SignOPT	Label	$\ell_2$	337	67.1	1.91
PointWise	Label	Optimized	4516	84.5	2.18
SparseEvo	Label	Optimized	9632	87.4	1.85
CA (sssp)	Label	Optimized	259	9.8	2.77
CA (bin search)	Label	Optimized	416	10.6	2.75

**Table 24: Attack performance under RAND Pre-processing Defense on WRN and CIFAR10 (Clean Accuracy: 92.6%)**

Attack	Query Type	Perturbation Type	# Query	Model Acc.	Dist. $\ell_2$
Bandit	Score	$\ell_\infty$	55	28.0	4.92
NES	Score	$\ell_\infty$	600	51.6	1.78
Parsimonious	Score	$\ell_\infty$	695	71.4	5.04
Sign	Score	$\ell_\infty$	627	70.6	4.82
Square	Score	$\ell_\infty$	142	28.6	5.00
ZOSignSGD	Score	$\ell_\infty$	642	52.3	1.80
GeoDA	Label	$\ell_\infty$	202	60.1	2.54
HSJ	Label	$\ell_\infty$	468	61.4	2.30
Opt	Label	$\ell_\infty$	1009	90.5	0.24
RayS	Label	$\ell_\infty$	454	69.2	4.62
SignFlip	Label	$\ell_\infty$	280	52.4	3.04
SignOPT	Label	$\ell_\infty$	1145	86.4	0.28
Bandit	Score	$\ell_2$	616	77.1	3.22
NES	Score	$\ell_2$	2074	77.0	0.82
Simple	Score	$\ell_2$	1639	92.0	0.15
Square	Score	$\ell_2$	62	30.9	4.57
ZOSignSGD	Score	$\ell_2$	2982	82.0	0.68
Boundary	Label	$\ell_2$	36	56.1	2.53
GeoDA	Label	$\ell_2$	191	60.9	2.35
HSJ	Label	$\ell_2$	627	57.2	2.97
Opt	Label	$\ell_2$	759	73.5	1.69
SignOPT	Label	$\ell_2$	527	60.5	2.34
PointWise	Label	Optimized	3721	87.2	1.90
SparseEvo	Label	Optimized	9730	89.7	1.7
CA (sssp)	Label	Optimized	401	6.1	3.63
CA (bin search)	Label	Optimized	461	0.0	4.80

**Table 25: Attack performance under RAND Pre-processing Defense on VGG and CIFAR100 (Clean Accuracy: 61.4%)**

Attack	Query Type	Perturbation Type	# Query	Model Acc.	Dist. $\ell_2$
Bandit	Score	$\ell_\infty$	9	8.8	3.28
NES	Score	$\ell_\infty$	326	34.4	0.91
Parsimonious	Score	$\ell_\infty$	218	37.1	3.26
Sign	Score	$\ell_\infty$	138	32.5	3.26
Square	Score	$\ell_\infty$	25	9.0	3.31
ZOSignSGD	Score	$\ell_\infty$	376	32.9	0.93
GeoDA	Label	$\ell_\infty$	139	40.5	2.36
HSJ	Label	$\ell_\infty$	301	43.7	2.12
Opt	Label	$\ell_\infty$	908	66.1	0.38
RayS	Label	$\ell_\infty$	127	46.4	4.03
SignFlip	Label	$\ell_\infty$	194	43.9	2.64
SignOPT	Label	$\ell_\infty$	997	60.3	0.46
Bandit	Score	$\ell_2$	187	43.9	1.43
NES	Score	$\ell_2$	1215	48.5	0.39
Simple	Score	$\ell_2$	1335	60.4	0.09
Square	Score	$\ell_2$	37	10.0	2.99
ZOSignSGD	Score	$\ell_2$	1804	54.8	0.33
Boundary	Label	$\ell_2$	26	41.0	2.48
GeoDA	Label	$\ell_2$	150	43.5	2.20
HSJ	Label	$\ell_2$	278	46.3	2.41
Opt	Label	$\ell_2$	765	56.5	1.44
SignOPT	Label	$\ell_2$	390	51.1	1.93
PointWise	Label	Optimized	956	51.3	1.07
SparseEvo	Label	Optimized	8793	53.2	0.95
CA (sssp)	Label	Optimized	168	0.9	2.25
CA (bin search)	Label	Optimized	457	0.0	2.52

**Table 26: Attack performance under RAND Pre-processing Defense on ResNet and CIFAR100 (Clean Accuracy: 62.4%)**

Attack	Query Type	Perturbation Type	# Query	Model Acc.	Dist. $\ell_2$
Bandit	Score	$\ell_\infty$	13	10.2	3.36
NES	Score	$\ell_\infty$	279	36.4	0.92
Parsimonious	Score	$\ell_\infty$	85	31.5	3.39
Sign	Score	$\ell_\infty$	221	33.1	3.33
Square	Score	$\ell_\infty$	12	9.7	3.48
ZOSignSGD	Score	$\ell_\infty$	330	34.9	0.94
GeoDA	Label	$\ell_\infty$	220	40.5	2.34
HSJ	Label	$\ell_\infty$	472	43.6	2.17
Opt	Label	$\ell_\infty$	907	62.7	0.32
RayS	Label	$\ell_\infty$	119	44.0	3.97
SignFlip	Label	$\ell_\infty$	383	40.0	2.93
SignOPT	Label	$\ell_\infty$	912	57.9	0.43
Bandit	Score	$\ell_2$	291	47.8	1.47
NES	Score	$\ell_2$	964	51.0	0.36
Simple	Score	$\ell_2$	1152	62.8	0.09
Square	Score	$\ell_2$	6	10.0	3.05
ZOSignSGD	Score	$\ell_2$	1514	55.2	0.30
Boundary	Label	$\ell_2$	16	37.7	2.52
GeoDA	Label	$\ell_2$	256	44.3	2.14
HSJ	Label	$\ell_2$	381	43.8	2.56
Opt	Label	$\ell_2$	806	54.5	1.46
SignOPT	Label	$\ell_2$	452	46.0	1.96
PointWise	Label	Optimized	2051	52.4	1.21
SparseEvo	Label	Optimized	9043	56.3	1.12
CA (sssp)	Label	Optimized	167	1.6	2.27
CA (bin search)	Label	Optimized	459	0.0	2.81

**Table 27: Attack performance under RAND Pre-processing Defense on ResNeXt and CIFAR100 (Clean Accuracy: 65.0%)**

Attack	Query Type	Perturbation Type	# Query	Model Acc.	Dist. $\ell_2$
Bandit	Score	$\ell_\infty$	20	9.2	3.43
NES	Score	$\ell_\infty$	311	35.3	0.95
Parsimonious	Score	$\ell_\infty$	359	40.7	3.54
Sign	Score	$\ell_\infty$	309	38.2	3.44
Square	Score	$\ell_\infty$	14	8.1	3.45
ZOSignSGD	Score	$\ell_\infty$	348	33.2	0.97
GeoDA	Label	$\ell_\infty$	152	48.6	2.06
HSJ	Label	$\ell_\infty$	184	51.3	1.94
Opt	Label	$\ell_\infty$	951	73.9	0.44
RayS	Label	$\ell_\infty$	203	56.7	4.23
SignFlip	Label	$\ell_\infty$	132	49.3	2.32
SignOPT	Label	$\ell_\infty$	798	71.8	0.45
Bandit	Score	$\ell_2$	188	45.7	1.49
NES	Score	$\ell_2$	1117	54.3	0.41
Simple	Score	$\ell_2$	1607	65.1	0.09
Square	Score	$\ell_2$	31	13.9	3.19
ZOSignSGD	Score	$\ell_2$	1964	58.3	0.35
Boundary	Label	$\ell_2$	17	49.7	2.21
GeoDA	Label	$\ell_2$	118	52.3	2.00
HSJ	Label	$\ell_2$	301	51.9	2.19
Opt	Label	$\ell_2$	741	65.1	1.35
SignOPT	Label	$\ell_2$	399	56.7	1.76
PointWise	Label	Optimized	1884	55.9	1.20
SparseEvo	Label	Optimized	9364	61.2	1.03
<b>CA (sssp)</b>	Label	Optimized	159	1.4	2.21
<b>CA (bin search)</b>	Label	Optimized	459	0.0	2.43

**Table 28: Attack performance under RAND Pre-processing Defense on WRN and CIFAR100 (Clean Accuracy: 65.5%)**

Attack	Query Type	Perturbation Type	# Query	Model Acc.	Dist. $\ell_2$
Bandit	Score	$\ell_\infty$	12	11.1	3.52
NES	Score	$\ell_\infty$	334	36.9	0.98
Parsimonious	Score	$\ell_\infty$	282	43.2	3.60
Sign	Score	$\ell_\infty$	144	43.9	3.51
Square	Score	$\ell_\infty$	21	11.9	3.57
ZOSignSGD	Score	$\ell_\infty$	383	36.9	0.99
GeoDA	Label	$\ell_\infty$	136	52.1	2.21
HSJ	Label	$\ell_\infty$	312	52.1	2.09
Opt	Label	$\ell_\infty$	866	74.4	0.37
RayS	Label	$\ell_\infty$	212	56.1	4.07
SignFlip	Label	$\ell_\infty$	146	50.0	2.47
SignOPT	Label	$\ell_\infty$	929	69.6	0.39
Bandit	Score	$\ell_2$	175	50.2	1.53
NES	Score	$\ell_2$	1131	55.3	0.41
Simple	Score	$\ell_2$	1268	65.2	0.09
Square	Score	$\ell_2$	20	13.1	3.19
ZOSignSGD	Score	$\ell_2$	1702	57.2	0.34
Boundary	Label	$\ell_2$	19	48.1	2.49
GeoDA	Label	$\ell_2$	171	50.7	2.17
HSJ	Label	$\ell_2$	250	50.3	2.34
Opt	Label	$\ell_2$	753	65.7	1.39
SignOPT	Label	$\ell_2$	395	56.0	1.81
PointWise	Label	Optimized	1617	55.1	1.07
SparseEvo	Label	Optimized	9157	59.1	0.85
<b>CA (sssp)</b>	Label	Optimized	180	1.2	2.37
<b>CA (bin search)</b>	Label	Optimized	457	0.0	2.49

**Table 29: Attack performance under RAND Post-processing Defense on VGG and CIFAR10 (Clean Accuracy: 90.5%)**

Attack	Query Type	Perturbation Type	# Query	Model Acc.	Dist. $\ell_2$
Bandit	Score	$\ell_\infty$	192	10.9	4.83
NES	Score	$\ell_\infty$	364	0.0	1.43
Parsimonious	Score	$\ell_\infty$	215	8.8	4.90
Sign	Score	$\ell_\infty$	134	1.2	4.88
Square	Score	$\ell_\infty$	37	0.4	4.89
ZOSignSGD	Score	$\ell_\infty$	389	0.1	1.40
GeoDA	Label	$\ell_\infty$	371	52.9	2.69
HSJ	Label	$\ell_\infty$	518	53.7	2.43
Opt	Label	$\ell_\infty$	970	78.0	0.31
RayS	Label	$\ell_\infty$	235	45.0	4.77
SignFlip	Label	$\ell_\infty$	76	17.2	3.91
SignOPT	Label	$\ell_\infty$	1177	34.2	1.13
Bandit	Score	$\ell_2$	999	25.6	3.78
NES	Score	$\ell_2$	1137	0.1	0.59
Simple	Score	$\ell_2$	3138	67.1	0.21
Square	Score	$\ell_2$	41	0.2	4.47
ZOSignSGD	Score	$\ell_2$	1955	1.6	0.53
Boundary	Label	$\ell_2$	57	52.3	2.14
GeoDA	Label	$\ell_2$	545	52.7	2.69
HSJ	Label	$\ell_2$	234	45.4	2.90
Opt	Label	$\ell_2$	641	53.3	2.02
SignOPT	Label	$\ell_2$	504	34.8	2.00
PointWise	Label	Optimized	1290	89.8	2.02
SparseEvo	Label	Optimized	9425	38.3	2.27
<b>CA (sssp)</b>	Label	Optimized	400	5.7	3.75
<b>CA (bin search)</b>	Label	Optimized	473	0.0	5.19

**Table 30: Attack performance under RAND Post-processing Defense on ResNet and CIFAR10 (Clean Accuracy: 92.0%)**

Attack	Query Type	Perturbation Type	# Query	Model Acc.	Dist. $\ell_2$
Bandit	Score	$\ell_\infty$	153	10.3	4.93
NES	Score	$\ell_\infty$	277	0.0	1.39
Parsimonious	Score	$\ell_\infty$	104	0.2	5.01
Sign	Score	$\ell_\infty$	144	0.7	4.98
Square	Score	$\ell_\infty$	18	0.0	4.99
ZOSignSGD	Score	$\ell_\infty$	274	0.0	1.35
GeoDA	Label	$\ell_\infty$	380	60.2	2.71
HSJ	Label	$\ell_\infty$	792	60.7	2.21
Opt	Label	$\ell_\infty$	658	84.9	0.21
RayS	Label	$\ell_\infty$	252	46.8	4.79
SignFlip	Label	$\ell_\infty$	442	17.0	4.26
SignOPT	Label	$\ell_\infty$	1095	42.0	1.00
Bandit	Score	$\ell_2$	673	20.7	3.76
NES	Score	$\ell_2$	840	0.0	0.54
Simple	Score	$\ell_2$	-	-	-
Square	Score	$\ell_2$	19	0.0	4.55
ZOSignSGD	Score	$\ell_2$	1443	0.1	0.47
Boundary	Label	$\ell_2$	85	64.4	1.68
GeoDA	Label	$\ell_2$	545	57.6	2.54
HSJ	Label	$\ell_2$	558	48.5	3.32
Opt	Label	$\ell_2$	593	59.4	1.98
SignOPT	Label	$\ell_2$	397	41.3	1.90
PointWise	Label	Optimized	1735	91.1	1.90
SparseEvo	Label	Optimized	8665	63.2	2.41
<b>CA (sssp)</b>	Label	Optimized	425	9.1	3.90
<b>CA (bin search)</b>	Label	Optimized	421	10.7	4.09

**Table 31: Attack performance under RAND Post-processing Defense on ResNeXt and CIFAR10 (Clean Accuracy: 94.8%)**

Attack	Query Type	Perturbation Type	# Query	Model Acc.	Dist. $\ell_2$
Bandit	Score	$\ell_\infty$	141	4.7	5.08
NES	Score	$\ell_\infty$	237	0.0	1.32
Parsimonious	Score	$\ell_\infty$	221	2.1	5.15
Sign	Score	$\ell_\infty$	133	0.0	5.14
Square	Score	$\ell_\infty$	23	0.4	5.14
ZOSignSGD	Score	$\ell_\infty$	249	0.0	1.31
GeoDA	Label	$\ell_\infty$	282	53.1	2.52
HSJ	Label	$\ell_\infty$	417	57.4	2.41
Opt	Label	$\ell_\infty$	683	81.6	0.36
RayS	Label	$\ell_\infty$	484	52.5	4.72
SignFlip	Label	$\ell_\infty$	287	28.1	3.35
SignOPT	Label	$\ell_\infty$	760	45.3	0.91
Bandit	Score	$\ell_2$	574	14.2	3.69
NES	Score	$\ell_2$	694	0.0	0.50
Simple	Score	$\ell_2$	4075	61.7	0.29
Square	Score	$\ell_2$	22	0.0	4.68
ZOSignSGD	Score	$\ell_2$	1459	0.6	0.47
Boundary	Label	$\ell_2$	20	51.1	2.36
GeoDA	Label	$\ell_2$	206	54.5	2.48
HSJ	Label	$\ell_2$	414	48.6	2.84
Opt	Label	$\ell_2$	542	61.2	1.70
SignOPT	Label	$\ell_2$	357	44.2	1.50
PointWise	Label	Optimized	2519	94.6	2.05
SparseEvo	Label	Optimized	9537	78.4	2.85
<b>CA (sssp)</b>	Label	Optimized	276	9.3	2.92
<b>CA (bin search)</b>	Label	Optimized	434	10.0	3.05

**Table 32: Attack performance under RAND Post-processing Defense on WRN and CIFAR10 (Clean Accuracy: 96.1%)**

Attack	Query Type	Perturbation Type	# Query	Model Acc.	Dist. $\ell_2$
Bandit	Score	$\ell_\infty$	157	6.2	5.12
NES	Score	$\ell_\infty$	464	0.2	1.59
Parsimonious	Score	$\ell_\infty$	390	21.1	5.22
Sign	Score	$\ell_\infty$	330	12.4	5.02
Square	Score	$\ell_\infty$	36	0.5	5.21
ZOSignSGD	Score	$\ell_\infty$	464	0.4	1.56
GeoDA	Label	$\ell_\infty$	186	56.9	2.58
HSJ	Label	$\ell_\infty$	364	56.0	2.37
Opt	Label	$\ell_\infty$	1022	84.8	0.31
RayS	Label	$\ell_\infty$	334	51.5	4.81
SignFlip	Label	$\ell_\infty$	164	22.8	3.72
SignOPT	Label	$\ell_\infty$	968	39.2	0.98
Bandit	Score	$\ell_2$	727	17.5	3.81
NES	Score	$\ell_2$	1328	1.6	0.68
Simple	Score	$\ell_2$	2536	74.7	0.21
Square	Score	$\ell_2$	26	0.4	4.75
ZOSignSGD	Score	$\ell_2$	2143	5.5	0.60
Boundary	Label	$\ell_2$	35	54.0	2.35
GeoDA	Label	$\ell_2$	267	58.3	2.53
HSJ	Label	$\ell_2$	360	48.8	2.82
Opt	Label	$\ell_2$	620	59.7	1.89
SignOPT	Label	$\ell_2$	476	43.4	1.65
PointWise	Label	Optimized	1727	95.8	1.89
SparseEvo	Label	Optimized	9720	59.9	2.67
<b>CA (sssp)</b>	Label	Optimized	399	7.3	3.65
<b>CA (bin search)</b>	Label	Optimized	460	0.0	4.94

**Table 33: Attack performance under RAND Post-processing Defense on VGG and CIFAR100 (Clean Accuracy: 68.5%)**

Attack	Query Type	Perturbation Type	# Query	Model Acc.	Dist. $\ell_2$
Bandit	Score	$\ell_\infty$	35	1.0	3.67
NES	Score	$\ell_\infty$	190	0.2	0.83
Parsimonious	Score	$\ell_\infty$	103	2.0	3.71
Sign	Score	$\ell_\infty$	72	0.7	3.66
Square	Score	$\ell_\infty$	8	0.1	3.66
ZOSignSGD	Score	$\ell_\infty$	203	0.1	0.82
GeoDA	Label	$\ell_\infty$	177	35.6	2.31
HSJ	Label	$\ell_\infty$	235	36.7	2.19
Opt	Label	$\ell_\infty$	756	53.3	0.48
RayS	Label	$\ell_\infty$	116	32.2	4.14
SignFlip	Label	$\ell_\infty$	40	14.4	2.89
SignOPT	Label	$\ell_\infty$	724	29.4	0.93
Bandit	Score	$\ell_2$	139	2.3	1.86
NES	Score	$\ell_2$	650	0.1	0.33
Simple	Score	$\ell_2$	2570	34.7	0.18
Square	Score	$\ell_2$	6	0.1	3.35
ZOSignSGD	Score	$\ell_2$	1225	0.5	0.30
Boundary	Label	$\ell_2$	40	28.8	2.31
GeoDA	Label	$\ell_2$	205	36.3	2.31
HSJ	Label	$\ell_2$	169	32.8	2.11
Opt	Label	$\ell_2$	581	37.7	1.54
SignOPT	Label	$\ell_2$	409	27.1	1.32
PointWise	Label	Optimized	494	67.5	1.38
SparseEvo	Label	Optimized	8502	21.1	1.75
<b>CA (sssp)</b>	Label	Optimized	186	1.8	2.35
<b>CA (bin search)</b>	Label	Optimized	582	0.0	2.67

**Table 34: Attack performance under RAND Post-processing Defense on ResNet and CIFAR100 (Clean Accuracy: 67.5%)**

Attack	Query Type	Perturbation Type	# Query	Model Acc.	Dist. $\ell_2$
Bandit	Score	$\ell_\infty$	46	1.0	3.57
NES	Score	$\ell_\infty$	152	0.0	0.75
Parsimonious	Score	$\ell_\infty$	56	0.0	3.63
Sign	Score	$\ell_\infty$	39	0.0	3.57
Square	Score	$\ell_\infty$	7	0.0	3.61
ZOSignSGD	Score	$\ell_\infty$	159	0.0	0.72
GeoDA	Label	$\ell_\infty$	245	38.7	2.49
HSJ	Label	$\ell_\infty$	407	38.2	2.28
Opt	Label	$\ell_\infty$	762	51.6	0.47
RayS	Label	$\ell_\infty$	99	32.7	4.03
SignFlip	Label	$\ell_\infty$	47	17.5	3.25
SignOPT	Label	$\ell_\infty$	839	28.2	0.97
Bandit	Score	$\ell_2$	211	3.2	1.86
NES	Score	$\ell_2$	431	0.0	0.28
Simple	Score	$\ell_2$	3593	36.0	0.20
Square	Score	$\ell_2$	6	0.0	3.28
ZOSignSGD	Score	$\ell_2$	791	0.0	0.24
Boundary	Label	$\ell_2$	56	34.2	2.35
GeoDA	Label	$\ell_2$	387	35.6	2.38
HSJ	Label	$\ell_2$	197	33.2	2.40
Opt	Label	$\ell_2$	633	40.2	1.60
SignOPT	Label	$\ell_2$	413	27.0	1.53
PointWise	Label	Optimized	922	65.7	1.41
SparseEvo	Label	Optimized	9028	41.0	2.02
<b>CA (sssp)</b>	Label	Optimized	187	1.8	2.36
<b>CA (bin search)</b>	Label	Optimized	458	0.0	3.04

**Table 35: Attack performance under RAND Post-processing Defense on ResNeXt and CIFAR100 (Clean Accuracy: 79.5%)**

Attack	Query Type	Perturbation Type	# Query	Model Acc.	Dist. $\ell_2$
Bandit	Score	$\ell_\infty$	46	1.3	4.28
NES	Score	$\ell_\infty$	165	0.0	0.92
Parsimonious	Score	$\ell_\infty$	117	0.5	4.33
Sign	Score	$\ell_\infty$	124	0.1	4.29
Square	Score	$\ell_\infty$	8	0.1	4.32
ZOSignSGD	Score	$\ell_\infty$	179	0.0	0.93
GeoDA	Label	$\ell_\infty$	147	40.7	2.04
HSJ	Label	$\ell_\infty$	201	41.4	1.91
Opt	Label	$\ell_\infty$	744	64.2	0.52
RayS	Label	$\ell_\infty$	179	45.7	4.32
SignFlip	Label	$\ell_\infty$	98	29.2	2.47
SignOPT	Label	$\ell_\infty$	844	43.8	0.86
Bandit	Score	$\ell_2$	163	3.1	2.03
NES	Score	$\ell_2$	461	0.0	0.34
Simple	Score	$\ell_2$	3805	45.2	0.23
Square	Score	$\ell_2$	10	0.0	3.90
ZOSignSGD	Score	$\ell_2$	1054	0.0	0.33
Boundary	Label	$\ell_2$	20	36.6	2.15
GeoDA	Label	$\ell_2$	143	44.3	2.02
HSJ	Label	$\ell_2$	256	40.6	2.13
Opt	Label	$\ell_2$	590	49.5	1.39
SignOPT	Label	$\ell_2$	371	38.0	1.56
PointWise	Label	Optimized	1811	78.7	1.75
SparseEvo	Label	Optimized	9476	62.6	2.20
CA (sssp)	Label	Optimized	179	2.0	2.33
CA (bin search)	Label	Optimized	458	0.0	2.60

**Table 36: Attack performance under RAND Post-processing Defense on WRN and CIFAR100 (Clean Accuracy: 79.4%)**

Attack	Query Type	Perturbation Type	# Query	Model Acc.	Dist. $\ell_2$
Bandit	Score	$\ell_\infty$	35	1.8	4.26
NES	Score	$\ell_\infty$	170	0.0	0.89
Parsimonious	Score	$\ell_\infty$	134	1.1	4.26
Sign	Score	$\ell_\infty$	81	0.6	4.24
Square	Score	$\ell_\infty$	10	0.0	4.23
ZOSignSGD	Score	$\ell_\infty$	178	0.1	0.89
GeoDA	Label	$\ell_\infty$	146	40.9	2.22
HSJ	Label	$\ell_\infty$	224	42.3	2.03
Opt	Label	$\ell_\infty$	738	62.1	0.46
RayS	Label	$\ell_\infty$	168	41.9	4.22
SignFlip	Label	$\ell_\infty$	50	24.1	2.70
SignOPT	Label	$\ell_\infty$	761	36.2	0.89
Bandit	Score	$\ell_2$	172	3.6	2.10
NES	Score	$\ell_2$	523	0.1	0.34
Simple	Score	$\ell_2$	2954	37.9	0.21
Square	Score	$\ell_2$	15	0.0	3.89
ZOSignSGD	Score	$\ell_2$	1009	0.7	0.32
Boundary	Label	$\ell_2$	25	35.6	2.34
GeoDA	Label	$\ell_2$	179	42.8	2.21
HSJ	Label	$\ell_2$	214	38.0	2.18
Opt	Label	$\ell_2$	597	46.7	1.41
SignOPT	Label	$\ell_2$	397	35.0	1.37
PointWise	Label	Optimized	1145	77.1	1.50
SparseEvo	Label	Optimized	9145	49.3	1.94
CA (sssp)	Label	Optimized	210	1.6	2.53
CA (bin search)	Label	Optimized	457	0.0	2.65

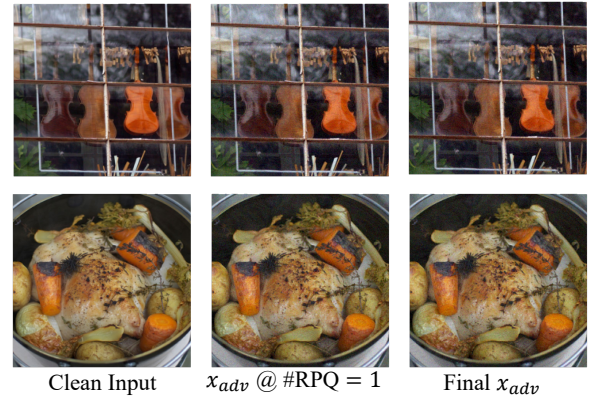


**Figure 7: Visualization of Successful Adversarial Examples Crafting by Certifiable Attack with SSSP Localization (SSSP requires fewer # RPQ)**

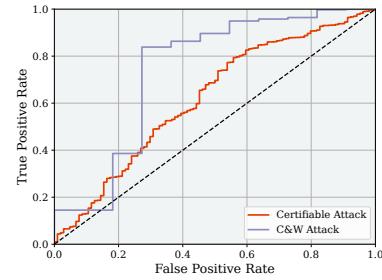


**Figure 8: ROC Curve of Detection Results by Feature Squeezing on CIFAR10. The ROC score is 0.38 and 0.26 for the C&W attack and certifiable attack, respectively**

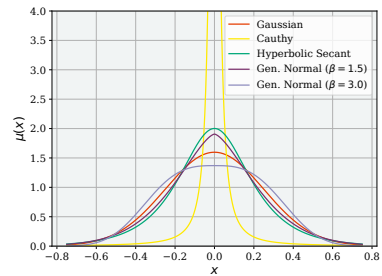


**Figure 9: PDF of Different Noise Distributions ( $\sigma = 0.25$ )**

**Table 37: RS-based defense against our attack on CIFAR10.  $\sigma = 0.25, p = 90\%$**

Defense Para.	Dist. $\ell_2$	Mean Dist. $\ell_2$	# RPQ	Cert. Acc.
none	12.95	2.34	14.35	91.21%
$\sigma_{r_s} = 0.12$	13.93	6.72	23.93	88.40%
$\sigma_{r_s} = 0.25$	16.07	11.84	33.93	87.20%
$\sigma_{r_s} = 0.50$	15.84	10.12	29.57	90.60%

## D.5 Experiments on Audio Classification task

**Dataset.** The speaker verification task focuses on determining if a given voice sample belongs to a specific individual or ascribed identity [10]. The process for this task entails comparing two voice



**Table 38: Performance of Certifiable Black-box Attack with Diffusion Denoise ( $p = 90\%$ ,  $\sigma = 0.25$ ). Diffusion Denoise can significantly reduce the perturbation size when the noise scale is very large.**

Dataset	denoise	Dist. $\ell_2$	Mean Dist. $\ell_2$	# RPQ	Certified Acc.
CIFAR10	w/o	12.95	2.34	14.35	91.21%
	w/	9.04	10.38	30.89	91.30%
ImageNet	w/o	24.32	0.72	5.60	99.8%
	w/	8.48	7.30	12.85	100.00%

samples using a speaker verification model and making a decision. We utilize the large-scale multi-speaker corpus LibriSpeech (“train-clean-100” set), which comprises over 100 hours of read English voices from 251 speakers encompassing various accents, occupations, and age groups. Within this corpus, each speaker has multiple voice samples spanning from several seconds to tens of seconds, sampled at a rate of 16kHz.

**Model and Setting.** For the speaker verification task, we use two SOTA speaker verification models: ECAPA-TDNN [23] pre-trained by Speechbrain [63] as the target model for the model owner and the X-vector model [29] pre-trained by Speechbrain [63] as the feature extractor. In the experiments, we utilize the pre-trained SOTA model, which is trained on the VoxCeleb dataset [57] and VoxCeleb2 dataset [21], to perform the task of verifying if two voice samples are from the same speaker. We evaluate the performance of the model on 500 pairs of voice samples randomly selected from the LibriSpeech “train-clean-100” set. Each sample pair consists of two voice samples from a single speaker.

**Table 39: Performance of certifiable attack with Gaussian Noise on Audio Dataset. ( $p = 90\%$ )**

$\sigma$	Dist. $\ell_2$	Mean Dist. $\ell_2$	# RPQ	Certified Acc.
0.05	18.35	12.67	5.42	100.00%
0.1	26.71	12.70	3.72	100.00%
0.15	35.82	12.63	3.12	100.00%

**Table 40: Performance of certifiable attack with Gaussian noise  $\sigma = 0.25$  on LibriSpeech**

p	Dist. $\ell_2$	Mean Dist. $\ell_2$	# RPQ	Certified Acc.
50%	26.64	12.55	5.31	100.00%
60%	26.65	12.57	5.08	100.00%
70%	26.66	12.60	4.87	100.00%
80%	26.68	12.63	4.49	100.00%
90%	26.71	12.70	3.72	100.00%
95%	26.74	12.78	3.05	100.00%

**Table 41: Attack performance of different localization/refinement algorithms on LibriSpeech ( $\sigma = 0.25$ ,  $p = 90\%$ ).**

Localization	Shifting	Dist. $\ell_2$	Mean Dist. $\ell_2$	# RPQ	Cert. Acc.
random	none	165.56	164.59	1.00	100.00%
random	geo.	159.21	157.53	73.88	100.00%
SSSP	none	26.72	12.74	1.32	100.00%
SSSP	geo.	26.71	12.70	3.72	100.00%